Bioorganic & Medicinal Chemistry 23 (2015) 5999–6013

Contents lists available at ScienceDirect

Bioorganic & Medicinal Chemistry

journal homepage: www.elsevier.com/locate/bmc

Vinyl sulfone analogs of lysophosphatidylcholine irreversibly inhibit autotaxin and prevent angiogenesis in melanoma

Mandi M. Murph [a,*,†], Guowei W. Jiang [b,†], Molly K. Altman [a], Wei Jia [a], Duy T. Nguyen [a], Jada M. Fambrough [a], William J. Hardman [c], Ha T. Nguyen [a], Sterling K. Tran [a], Ali A. Alshamrani [a], Damian Madan [d], Jianxing Zhang [b], Glenn D. Prestwich [b,*]

[a] Department of Pharmaceutical and Biomedical Sciences, The University of Georgia, College of Pharmacy, 240 W. Green Street, Athens, GA 30602, United States
[b] Department of Medicinal Chemistry, The University of Utah, 419 Wakara Way, Suite 205, Salt Lake City, UT 84108-1257, United States
[c] The University of Georgia and Georgia Regents University Medical Partnership, 1425 Prince Avenue, Athens, GA 30606, United States
[d] Echelon Biosciences Incorporated, 675 Arapeen Way, Suite 302, Salt Lake City, UT 84108, United States

ARTICLE INFO

Article history:
Received 31 March 2015
Revised 12 June 2015
Accepted 20 June 2015
Available online 2 July 2015

Keywords:
Angiogenesis
Anticancer therapy
Autotaxin
Lysophosphatidylcholine
Melanoma
Vinyl sulfone

ABSTRACT

Autotaxin (ATX) is an enzyme discovered in the conditioned medium of cultured melanoma cells and identified as a protein that strongly stimulates motility. This unique ectonucleotide pyrophosphatase and phosphodiesterase facilitates the removal of a choline headgroup from lysophosphatidylcholine (LPC) to yield lysophosphatidic acid (LPA), which is a potent lipid stimulator of tumorigenesis. Thus, ATX has received renewed attention because it has a prominent role in malignant progression with significant translational potential. Specifically, we sought to develop active site-targeted irreversible inhibitors as anti-cancer agents. Herein we describe the synthesis and biological activity of an LPC-mimetic electrophilic affinity label that targets the active site of ATX, which has a critical threonine residue that acts as a nucleophile in the lysophospholipase D reaction to liberate choline. We synthesized a set of quaternary ammonium derivative-containing vinyl sulfone analogs of LPC that function as irreversible inhibitors of ATX and inactivate the enzyme. The analogs were tested in cell viability assays using multiple cancer cell lines. The IC_{50} values ranged from 6.74 to 0.39 μM, consistent with a K_i of 3.50 μM for inhibition of ATX by the $C_{16}H_{33}$ vinyl sulfone analog CVS-16 (**10b**). A phenyl vinyl sulfone control compound, PVS-16, lacking the choline-like quaternary ammonium mimicking head group moiety, had little effect on cell viability and did not inhibit ATX. Most importantly, CVS-16 (**10b**) significantly inhibited melanoma progression in an in vivo tumor model by preventing angiogenesis. Taken together, this suggests that CVS-16 (**10b**) is a potent and irreversible ATX inhibitor with significant biological activity both in vitro and in vivo.

1. Introduction

The ectonucleotide pyrophosphatase/phosphodiesterase 2 or its more common designation autotaxin (ATX), is an enzyme with lysophospholipase D activity that converts lysophosphatidylcholine (LPC) to lysophosphatidic acid (LPA)[1] by hydrolysis of the choline head group from LPC. Although it is central to the biosynthesis of LPA, ATX also hydrolyzes *p*-nitrophenyl thymidine-5′-monophosphate, which is a type I phosphodiesterase substrate.[2] Thus, it is a multi-faceted enzyme with more than one important function.

ATX was isolated from conditioned medium of melanoma cells,[3] and was discovered to play a major role in the development of both the vascular[4] and nervous systems[5] as well as malignancy.[6] In particular, ATX promotes cancer progression, since it can increase growth factor signaling, cell survival, proliferation and migration in many cancers, including pancreatic cancer,[7] cutaneous and uveal melanoma,[8] breast cancer,[6b] follicular lymphoma,[9] glioblastoma multiforme[10] and gynecologic malignancies.[11] In addition, ATX protects cancer cells from chemotherapy-induced apoptosis,[12] which could significantly compromise cancer treatment and result in worsened outcomes when ATX is present in the tumor microenvironment.

Abbreviations: ATX, autotaxin; LPA, lysophosphatidic acid; LPC, lysophosphatidylcholine.

* Corresponding authors.
E-mail addresses: mmurph@uga.edu (M.M. Murph), gprestwich@pharm.utah.edu (G.D. Prestwich).

† These authors contributed equally to this research study.

http://dx.doi.org/10.1016/j.bmc.2015.06.054
0968-0896/

Another occurrence affecting cancer treatment is angiogenesis. This is the process whereby tumors develop blood vessels to access nutrients and oxygen from circulation and is necessary for tumor growth beyond 1 mm, a point at which necrosis occurs in otherwise hypoxic tissues. To state succinctly—angiogenesis is required for tumor progression. Without angiogenesis, the growing tumor will not thrive and will remain small. Because of this dependency, anticancer therapeutics targeting angiogenesis exploit tumors by inhibiting growth factors required for the formation of new blood vessels, such as the vascular endothelial growth factor (VEGF). Other growth factors, besides VEGF are secreted by the tumor when it exceeds a certain distance from its primary blood supply and senses hypoxia. On the other hand, since the circulatory system is exploited by intravenous anticancer therapeutics to reach the insides of tumors, timing is critical to properly treat patients with angiogenesis inhibitors.

Interestingly, ATX is a direct and indirect angiogenic factor that stimulates human endothelial cells to form tubules and tumors to become more hyperemic.[13] It is thus not surprising that the outcome of knocking out ATX on vasculogenesis results in embryonic lethal mutations in mice embryos which display aberrant blood vessel formation upon death.[4] Mechanistically, an increase in VEGF increases ATX expression and secretion among (at least) ovarian cancer cells. This resultant increase in ATX then results in more lysophosphatidic acid and also drives cells to produce more of the receptors LPA3, LPA4 and VEGFR2.[14] This represents a positive feedback loop between ATX and growth factors involved in angiogenesis, especially since lysophosphatidic acid also stimulates VEGF production. In other words, ATX plays a central role in angiogenesis and thus, tumor progression.

Because of the critical role ATX has in angiogenesis and various malignancies, extensive research is devoted to the design, synthesis and evaluation of novel inhibitors of ATX[8a,b,15] as well as the evaluation of natural substances with inhibitory activity.[16] Some recently designed chemical inhibitors have not possessed the necessary characteristics to proceed into clinical development due to a lack of bioavailability or large millimolar concentrations required for activity. Interestingly, ATX is product-inhibited by both sphingosine 1-phosphate and lysophosphatidic acid.[17] This suggests that these bioactive lipids are capable of regulating their own synthesis in the microenvironment and this knowledge bestows a scheme to chemically exploit their abundance. Other studies have elucidated the crystal structure of ATX[18] and further described how the enzyme discriminates substrates,[19] which resulted in novel ideas for the design of additional ATX inhibitors.

Herein we report the synthesis and biological testing of a series of alkyl vinyl sulfone analogs of LPC. These analogs feature a quaternary ammonium derivative, a reactive vinyl sulfone, and alkyl chains varying in length from C_6 to C_{18}. We also prepared a control compound, a phenyl vinyl sulfone, which lacked the targeting by the quaternary ammonium derivative but retained the long alkyl chain. Vinyl sulfone derivatives are widely known as irreversible inhibitors of cysteine proteases.[20] The mechanism of this irreversible inhibition depends on the vinyl sulfone acting as a Michael acceptor covalently reacting with the soft nucleophiles, such as thiols.[21] Studies indicate that peptide vinyl sulfone inhibitors also modify the active site threonine (Thr) of the *Escherichia coli* HsIV homolog and *Rhodococcus* proteasome.[21b,22] Similar to the inhibition of cysteine protease, the inhibition of proteasome by peptide vinyl sulfone also involves covalent modification of the *N*-terminal Thr of the catalytic β subunits, via a Michael addition.[21] Taken together, this suggested that vinyl sulfone might be an appropriate electrophile for targeting the active site Thr of ATX.

We hypothesized that the choline headgroup of ATX was an important recognition element for ATX, and would position the vinyl sulfone moiety in the active site in the vicinity of the Thr residue. A straight chain alkyl group was positioned in the 2-position of the vinyl sulfone, leaving a reactive, unsubstituted 1-position available to interact with an active site nucleophile. Several alkyl chains varying in length from C_6 to C_{18} were employed to identify the optimal analog. We proposed that the metal-activated hydroxyl group of the catalytic-site threonine could attack the vinyl sulfone and form a covalent bond that would irreversibly inactivate the enzyme.

Indeed, we observed that vinyl sulfone analogs could reduce in vitro cell viability, cell motility, wound closure and melanoma growth in vivo. We previously synthesized ATX inhibitors and examined their biological activity against melanoma[8a,b,23] and other malignancies.[15d,e,24] Since the in vitro activity observed by ATX inhibitors on melanoma cells is striking, we hypothesized that the mechanism of action is a directly-targeted, cellular consequence. However, we did not observe a direct effect against proliferation of melanoma models in vivo. Instead, the animal tumors treated with the highest compound concentration displayed significantly smaller tumors than controls, which resulted from an inhibition of angiogenesis, not mitogenesis. Herein we report the synthesis of novel vinyl sulfones and their action against the progression of melanoma via angiogenesis inhibition.

2. Materials and methods

2.1. General chemicals and spectroscopy

All synthetic reagent chemicals and solvents were purchased from Aldrich (St. Louis, MO), Alfa Aesar (Ward Hill, MA) or Acros Chemical Corporation (Geel, Belgium) and used without prior purification. Thin-layer chromatography was performed on precoated silica gel aluminum sheets (EM SCIENCE silica gel $60F_{254}$). Purification of compounds was carried out by normal phase chromatography (ISCO Combiflash, Silica gel 230–400 mesh). NMR spectra were recorded using a Varian Mercury 400 at 400 MHz (^{1}H), 101 MHz (^{13}C), 162 MHz (^{31}P), 376 MHz (^{19}F) at 25 °C. Chemical shifts are given in ppm with TMS as internal standard ($\delta = 0.00$); ^{31}P, 85% H_3PO_4 ($\delta = 0.00$). NMR peaks were assigned by MestRe-C (4.9.9.9). Low resolution mass spectra were obtained on HP5971A MSD double focusing mass spectrometer instrument. For biological studies, oleoyl (18:1) lysophosphatidic acid was purchased from Avanti Polar Lipids (Alabaster, AL) and reconstituted in chloroform and methanol. Prior to cell incubation, organic solutions were removed and ATX was added in 0.1% charcoal-stripped BSA.

2.2. Chemical synthesis of intermediates and final products

Ethyl 2-bromopropionate **2** (5 g, 36.0 mmol) was dissolved in acetone (200 mL), K_2CO_3 (7.45 g, 54.0 mmol, 1.5 equiv) was added, followed by of methyl-2 mercaptoacetate **1** (4.2 g, 39.5 mmol, 1.1 equiv) and heated at reflux for 2 h. After cooling to room temperature the mixture was filtered out, and then the white cake was washed with acetone (25 mL × 2). All combined organic solvents were evaporated under reduced pressure. The residue was purified on silica column (ethyl acetate–hexanes, 15–40%) to yield the pure product methyl 2-(3-hydroxypropylthio)acetate **3** (5.78 g, 35.3 mmol, 98%).

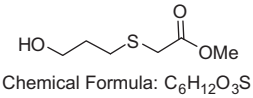

Chemical Formula: $C_6H_{12}O_3S$
Exact Mass: 164.0507
3

^{1}H NMR ($CDCl_3$) δ 3.67 (s, 3H), 3.66 (t, J = 6.0 Hz, 2H), 3.19 (s, 2H), 2.68 (t, J = 7.2 Hz, 2H), 2.54 (s, 1H), 1.78 (m, 2H); ^{13}C NMR ($CDCl_3$) δ 171.1 (s), 61.0 (s), 52.4 (s), 33.4 (s), 31.5 (s), 29.2 (s); MS (ESI) m/z 165.2 (M^++1).

Trityl chloride (3.34 g, 12 mmol), triethylamine (2.5 mL, 25 mmol) and the alcohol **3** (1.64 g, 10 mmol) was added to CH_2Cl_2 (100 mL). The reaction mixture was stirred at room temperature (rt) overnight. The reaction mixture was then washed twice with 5% $NaHCO_3$ (60 mL), followed by saturated NaCl solution (50 mL). The organic layer was dried over Na_2SO_4, solvents were removed by evaporation, and the residue was purified on silica column (ethyl acetate–hexanes, 0–10%) to yield the pure product, methyl 2-(3-(trityloxy)propylthio)acetate **4** (3.82 g, 9.4 mmol, 94%).

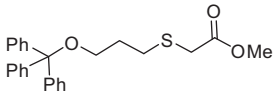

Chemical Formula: $C_{25}H_{26}O_3S$
Exact Mass: 406.1603

4

^{1}H NMR ($CDCl_3$) δ 7.41–7.45 (m, 6H), 7.20–7.33 (m, 9H), 3.71 (s, 3H), 3.20 (s, 2H), 3.16 (t, J = 6.0 Hz, 2H), 2.76 (t, J = 7.2 Hz, 2H), 1.89 (m, 2H); ^{13}C NMR ($CDCl_3$) δ 171.0 (s), 144.2 (s), 128.6 (s), 127.8 (s), 126.9 (s), 86.5 (s), 62.0 (s), 52.4 (s), 33.4 (s), 29.7 (d); MS (ESI) m/z 429.3 (M+Na^+).

The sulfide **4** (24.2 g, 59.7 mmol, 1 equiv) was dissolved in CH_2Cl_2 (300 mL) and *m*-CPBA (25.7 g, 149 mmol, 2.5 equiv) was added at 0 °C. The reaction mixture was allowed warm up to rt and stirred for 8 h at rt. Volatiles were evaporated under reduced pressure. The residue was taken up in ethyl acetate (200 mL) and washed with 10% Na_2SO_3, saturated $NaHCO_3$, and brine. The organic layer was then dried over anhydrous Na_2SO_4. The volatiles were evaporated under reduced pressure to yield the crude mixture that was purified on silica column (ethyl acetate–hexanes, 0–50%) to yield the pure product, methyl 2-(3-(trityloxy)propylsulfonyl)acetate **5** (24.8 g, 56.7 mmol, 95%).

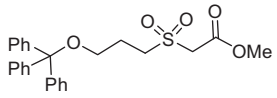

Chemical Formula: $C_{25}H_{26}O_5S$
Exact Mass: 438.1501

5

^{1}H NMR ($CDCl_3$) δ 7.41–7.51 (m, 6H), 7.20–7.38 (m, 9H), 3.97 (s, 2H), 3.81 (s, 3H), 3.38–3.46 (m, 2H), 2.29 (t, J = 5.6 Hz, 2H), 3.20 (s, 2H), 2.05–2.21 (m, 2H); ^{13}C NMR ($CDCl_3$) δ 163.5 (s), 143.9 (s), 128.6 (s), 128.0 (d), 127.9 (s), 127.2 (s), 86.9 (s), 61.3 (s), 57.2 (s), 53.4 (s), 51.3 (s), 22.9 (s); MS (ESI) m/z 439.3 (M^++H).

To a solution of 3.7 g (6.41 mmol, 1 equiv) of intermediate **5** in 20 mL of DMF was added sodium hydride (60% in mineral oil, 400 mg, 9.7 mmol, 1.15 equiv). The reaction mixture was then stirred at rt for 1 h before 3.82 g (10.2 mmol, 1.2 equiv) oleyl iodide in 10 mL DMF was added. The mixture was stirred additional 4 h before 1 N HCl (100 mL) was added to quench the reaction, and the mixture was extracted with 100 mL of ethyl ether. The combined organic extracts were washed with saturated $NaHCO_3$ solution, followed by a saturated NaCl solution. Solvents were removed at reduced pressure and the crude mixture was purified on silica column (ethyl acetate–hexanes, 0–20%) to give clear oil (*Z*)-methyl 2-(3-(trityloxy)propylsulfonyl)eicos-11-enoate **6a** (3.18 g, 4.61 mmol, 72%).

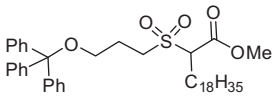

Chemical Formula: $C_{43}H_{60}O_5S$
Exact Mass: 688.4161

6a

^{1}H NMR ($CDCl_3$) δ 7.41–7.51 (m, 6H), 7.20–7.38 (m, 9H), 5.31–5.39 (m, 2H), 3.83 (s, 3H), 3.76–3.81 (m, 1H), 3.15–3.32 (m, 4H), 1.99–2.18 (m, 6H), 1.20–1.40 (m, 26H), 0.90 (t, J = 6.8 Hz, 3H); ^{13}C NMR ($CDCl_3$) δ 167.0 (s), 143.8 (s), 130.0 (s), 129.8 (s), 128.6 (s), 127.9 (d), 127.1 (s), 86.8 (s), 68.7 (s), 61.5 (s), 53.2 (s), 48.6 (s), 31.9 (s), 29.1–29.8 (m), 27.2 (m), 26.2 (s), 22.7 (s), 22.1 (s), 14.2 (s); MS (ESI) m/z 711.6 (M+Na^+).

A similar procedure for **6a** was followed, using hexadecyl iodide, to give methyl 2-(3-(trityloxy)propylsulfonyl)octadecanoate **6b** (6.1 g, 9.2 mmol, 88%).

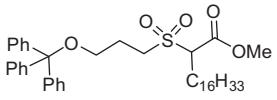

Chemical Formula: $C_{41}H_{58}O_5S$
Exact Mass: 662.4005

6b

^{1}H NMR ($CDCl_3$) δ 7.40–7.51 (m, 6H), 7.21–7.39 (m, 9H), 3.81 (s, 3H), 3.76–3.81 (m, 1H), 3.21–3.46 (m, 4H), 2.14–2.23 (m, 4H), 1.60–1.67 (m, 2H), 1.20–1.40 (m, 26H), 0.88 (t, J = 6.8 Hz, 3H); ^{13}C NMR ($CDCl_3$) δ 167.0 (s), 143.8 (s), 128.6 (s), 127.8 (d), 127.1 (s), 86.8 (s), 68.7 (s), 61.5 (s), 53.2 (s), 48.6 (s), 31.9 (s), 29.1–29.8 (m), 27.2 (m), 26.2 (s), 22.7 (s), 22.1 (s), 14.2 (s); MS (ESI) m/z 685.3 (M+Na^+).

To an ice-cooled solution of 800 mg (1.16 mmol, 1 equiv) of **6a** in 15 mL of THF was added 44 mg (1.16 mmol, 1.0 equiv) of lithium aluminum hydride. The reaction mixture was then stirred at 0 °C for 10 min. Next, 20 mL water was added dropwise to quench the reaction, and the mixture was extracted twice with 50 mL of ethyl acetate. The combined organic extracts were washed with 1 N HCl, saturated $NaHCO_3$ solution, and saturated NaCl solution. Solvents were removed at reduced pressure and the crude mixture was purified on silica column (ethyl acetate–hexanes, 5–25%) to give the product (*Z*)-2-(3-(trityloxy)propylsulfonyl)eicos-11-en-1-ol **7a** (390 mg, 0.59 mmol, 51%).

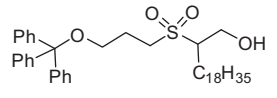

Chemical Formula: $C_{42}H_{60}O_4S$
Exact Mass: 660.4212

7a

^{1}H NMR ($CDCl_3$) δ 7.41–7.51 (m, 6H), 7.20–7.38 (m, 9H), 5.31–5.39 (m, 2H), 3.93–4.06 (m, 2H), 3.24 (t, J = 6.0 Hz, 2H), 3.11–3.17 (m, 2H), 2.92–3.00 (m, 1H), 2.57 (t, J = 6.0 Hz, 2H), 2.16–2.20 (m, 2H), 1.95–2.04 (m, 4H), 1.82–1.92 (m, 1H), 1.61–1.71 (m, 1H), 1.45–1.54 (m, 1H), 1.20–1.40 (m, 22H), 0.88 (t, J = 6.8 Hz, 3H); ^{13}C NMR ($CDCl_3$) δ 143.8 (s), 130.0 (s), 129.8 (s), 128.5 (s), 127.9 (s), 127.1 (s), 86.8 (s), 63.8 (s), 61.5 (s), 59.5 (s), 49.5 (s), 31.9 (s), 29.1–29.8 (m), 27.2 (d), 26.9 (s), 24.3 (s), 22.7 (s), 22.3 (s), 14.1 (s); MS (ESI) m/z 683.6 (M+Na^+).

Similarly, **6b** was reduced, worked up, and purified to give (trityloxy)propylsulfonyl)octadecan-1-ol **7b** (2.45 g, 3.86 mmol, 34%).

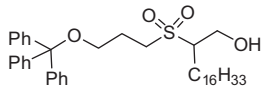

Chemical Formula: $C_{40}H_{58}O_4S$
Exact Mass: 634.4056

7b

^{1}H NMR ($CDCl_3$) δ 7.40–7.51 (m, 6H), 7.21–7.38 (m, 9H), 3.93–4.06 (m, 2H), 3.24 (t, J = 6.0 Hz, 2H), 3.11–3.17 (m, 2H), 2.92–3.00 (m, 2H), 2.57 (t, J = 6.0 Hz, 2H), 2.16–2.20 (m, 2H), 1.82–1.92 (m, 1H), 1.61–1.71 (m, 1H), 1.20–1.40 (m, 26H), 0.89 (t, J = 6.8 Hz, 3H); ^{13}C NMR ($CDCl_3$) δ 143.8 (s), 128.5 (s), 127.9 (s), 127.1 (s), 86.8 (s), 63.8 (s), 61.5 (s), 59.5 (s), 49.5 (s), 31.9 (s), 29.1–29.8 (m), 27.2 (d), 26.9 (s), 24.3 (s), 22.7 (s), 22.3 (s), 14.1 (s); MS (ESI) m/z 657.5 ($M+Na^+$).

To a solution of 330 mg (0.6 mmol, 1 equiv) of **7a** in 5 mL of CH_2Cl_2 was added 0.4 mL of trifluoroacetic acid. Next, the reaction mixture was stirred at rt for 30 min; 30 mL saturated $NaHCO_3$ solution was added to quench the reaction, and the mixture was extracted with three portions of 50 mL of ethyl acetate. The organic solvents were removed at reduced pressure and the crude mixture was purified on silica column (ethyl acetate–hexanes, 50–100%) to give the product (*Z*)-2-(3-hydroxypropylsulfonyl)eicos-11-en-1-ol **8a** (203 mg, 0.49 mmol, 81%).

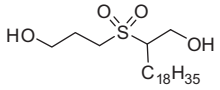

Chemical Formula: $C_{23}H_{46}O_4S$
Exact Mass: 418.3117

8a

^{1}H NMR ($CDCl_3$) δ 5.31–5.39 (m, 2H), 3.93–4.06 (m, 2H), 3.81 (t, J = 6.0 Hz, 2H), 3.22 (t, J = 7.2 Hz, 2H), 2.95–3.03 (m, 1H), 2.07–2.17 (m, 2H), 1.88–2.12 (m, 6H), 1.61–1.71 (m, 1H), 1.45–1.54 (m, 1H), 1.20–1.40 (m, 24H), 0.88 (t, J = 6.8 Hz, 3H); ^{13}C NMR ($CDCl_3$) δ 130.0 (s), 129.8 (s), 64.5 (s), 60.7 (s), 59.6 (s), 49.0 (s), 31.9 (s), 29.1–29.8 (m), 27.2 (d), 26.9 (s), 24.3 (s), 22.7 (s), 14.1 (s); MS (ESI) m/z 419.4 (M^++1).

Similarly, **7b** was deprotected was to give 2-(3-hydroxypropylthio)octadecan-1-ol **8b** (580 mg, 1.61 mmol, 66%).

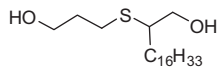

Chemical Formula: $C_{21}H_{44}O_2S$
Exact Mass: 360.3062

8b

^{1}H NMR ($CDCl_3$) δ 3.93–4.06 (m, 2H), 3.80 (t, J = 6.0 Hz, 2H), 3.21 (t, J = 7.6 Hz, 2H), 2.95–3.03 (m, 1H), 2.07–2.17 (m, 2H), 1.88–2.12 (m, 2H), 1.61–1.71 (m, 1H), 1.45–1.54 (m, 1H), 1.20–1.40 (m, 26H), 0.88 (t, J = 6.8 Hz, 3H); ^{13}C NMR ($CDCl_3$) δ 64.5 (s), 60.7 (s), 59.6 (s), 49.0 (s), 31.9 (s), 29.1–29.8 (m), 27.2 (d), 26.9 (s), 24.3 (s), 22.7 (s), 14.1 (s); MS (ESI) m/z 361.4 (M^++1).

The next protocols involve reaction of both primary alcohols and selective elimination to afford a vinyl sulfone in two steps. To a solution of 3.31 g (7.92 mmol, 1 equiv) of **8a** and diisopropyl ethylamine (5.1 g, 39.4 mmol, 5 equiv) in 40 mL of CH_2Cl_2 was added mesyl chloride (2.74 g, 19.0 mmol, 2.4 equiv). The reaction mixture was then stirred at rt for 2 h. The precipitate was removed by filtration, and the filtrate was washed with saturated $NaHCO_3$ solution and dried over sodium sulfate. The organic solvent was concentrated and the residue was dissolved into acetone (30 mL) followed by NaI (3.6 g, 16 mmol, 3 equiv) and $NaHCO_3$ (1.0 g, 11.9 mmol, 2.2 equiv). The reaction mixture was stirred at rt overnight, filtered out and concentrated by evaporation; then, 50 mL water and 50 mL ethyl acetate was added to the residue. The organic layer was collected, the aqueous layer was re-extracted twice with ethyl acetate, and the combined organics were dried over sodium sulfate and then removed at reduced pressure. Next, 100 mL ethyl acetate was added, followed by diisopropylethylamine (5 mL). The reaction mixture was stirred at rt for 3 days. The organic solvent was removed at reduced pressure and the crude mixture was purified on silica column (ethyl acetate–hexanes, 0–15%) to give the product (*Z*)-2-(3-iodopropylsulfonyl)eicosa-1,11-diene **9a** (3.27 g, 6.42 mmol, 81%).

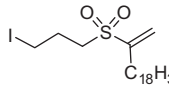

Chemical Formula: $C_{23}H_{43}IO_2S$
Exact Mass: 510.2028

9a

^{1}H NMR ($CDCl_3$) δ 6.25 (s, 1H), 5.83 (s, 1H), 5.31–5.40 (m, 2H), 3.28 (t, J = 6.4 Hz, 2H), 3.07 (t, J = 7.6 Hz, 2H), 2.41 (t, J = 7.6 Hz, 2H), 2.22–2.30 (m, 2H), 1.94–2.06 (m, 4H), 1.56–1.66 (m, 2H), 1.20–1.40 (m, 22H), 0.88 (t, J = 6.8 Hz, 3H); ^{13}C NMR ($CDCl_3$) δ 146.0 (s), 126.9 (s), 126.6 (s), 122.0 (s), 64.5 (s), 49.7 (s), 28.8 (s), 26.1–26.6 (m), 25.9 (s), 24.6 (s), 24.1 (d), 23.0 (s), 19.6 (s), 11.0 (s); MS (ESI) m/z 533.3 ($M+Na^+$).

A similar two-step procedure was employed using **8b** as the starting material to give 2-(3-iodopropylsulfonyl)octadec-1-ene **9b** (198 mg, 0.41 mmol, 45%).

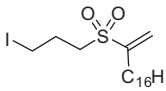

Chemical Formula: $C_{21}H_{41}IO_2S$
Exact Mass: 484.1872

9b

^{1}H NMR ($CDCl_3$) δ 6.18 (s, 1H), 5.77 (s, 1H), 3.22 (t, J = 6.4 Hz, 2H), 3.02 (m, 2H), 2.34 (t, J = 7.6 Hz, 2H), 2.14–2.23 (m, 2H), 1.50–1.58 (m, 2H), 1.56–1.66 (m, 2H), 1.20–1.40 (m, 24H), 0.81 (t, J = 6.8 Hz, 3H); ^{13}C NMR ($CDCl_3$) δ 145.6 (s), 122.0 (s), 49.5 (s), 28.7 (s), 26.0–26.4 (m), 25.8 (s), 24.4 (s), 22.9 (d), 19.5 (s), 10.9 (s); MS (ESI) m/z 507.3 ($M+Na^+$).

Next, the quaternary ammonium derivatives were introduced. To a solution of 81 mg (0.16 mmol, 1 equiv) of **9a** in 5 mL ethanol + 1 mL methylene chloride was added trimethylamine in ethanol. Then the reaction mixture was stirred at rt for 4 days. The resulting mixture was concentrated and then dissolved into 0.5 mL ethanol followed by adding 10 mL diethyl ether. The white solid precipitated and the white solid was collected by filtration to give the final product, which was passed through a chloride ion exchange resin to convert to (*Z*)-3-(eicosa-1,11-dien-2-ylsulfonyl)-*N*,*N*,*N*-trimethylpropan-1-aminium chloride CVS-18 (51 mg, 0.11 mmol, 71%).

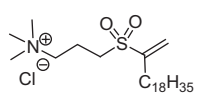

$C_{26}H_{52}ClNO_2S^-$
Exact Mass: 477.3413

10a in salt

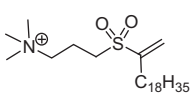

Chemical Formula: $C_{26}H_{52}NO_2S^+$
Exact Mass: 442.3713

10a

^{1}H NMR ($CDCl_3$) δ 6.26 (s, 1H), 5.88 (s, 1H), 5.85 (s, 1H), 5.31–5.40 (m, 2H), 3.98–4.40 (m, 2H), 3.59 (s, 3H), 3.45 (s, 9H), 3.18 (t, J = 6.8 Hz, 2H), 2.84 (d, J = 6.8 Hz, 2H), 2.34–2.43 (m, 4H), 1.57–1.62 (m, 2H), 1.32–1.42 (m, 22H), 0.87 (t, J = 6.8 Hz, 3H); ^{13}C NMR ($CDCl_3$) δ 149.1 (s), 130.0 (s), 129.7 (s), 125.6 (s), 64.5 (s), 53.7 (s), 52.0 (s), 48.6 (s), 44.9 (s), 31.9 (s), 29.0–29.7 (m),

27.7 (s), 27.2 (d), 22.6 (d), 16.5 (s), 14.1 (s); MS (ESI) *m*/*z* 442.5 (M^+).

A similar procedure for CVS-18 was used to give *N*,*N*,*N*-trimethyl-3-(octadec-1-en-2-ylsulfonyl)propan-1-aminium chloride CVS-16 (21 mg, 0.05 mmol, 85%).

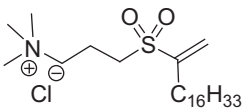

$C_{24}H_{50}ClNO_2S$
Exact Mass: 451.3251
10b in salt

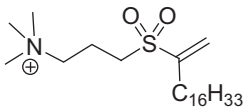

$C_{24}H_{50}NO_2S^+$
Exact Mass: 416.3557
10b

^{1}H NMR (CD_3OD) δ 6.25 (s, 1H), 5.98 (s, 1H), 3.48–4.55 (m, 2H), 3.26 (s, 2H), 3.16–3.22 (m, 11H), 2.45 (t, J = 7.6 Hz, 2H), 2.18–2.28 (m, 2H), 1.60–1.67 (m, 2H), 1.32–1.42 (m, 24H), 0.90 (t, J = 6.8 Hz, 3H); ^{13}C NMR (CD_3OD) δ 149.2 (s), 125.1 (s), 64.3 (s), 52.2 (m), 48.4 (s), 31.7 (s), 29.0–29.4 (m), 28.8 (s), 27.6 (s), 22.3 (d), 16.2 (s), 13.0 (s); MS (ESI) *m*/*z* 416.5 (M^+).

Modified protocols were required to prepare the two shorter chain analogs. Thus, bromo ester **12** (12.06 g, 36.0 mmol) was dissolved in acetone (200 mL), K_2CO_3 (7.45 g, 54.0 mmol, 1.5 equiv) was added, followed by of methyl 2-mercaptoacetate **11** (4.2 g, 39.5 mmol, 1.1 equiv) and heated at reflux for 2 h. After cooling to room temperature the mixture was filtered and the white solid was washed twice with 25 mL acetone. Combined organic solvents were evaporated under reduced pressure, and the residue was purified on silica column (ethyl acetate–hexanes, 15–40%) to yield the pure product ethyl 2-(3-methoxy-3-oxopropylthio)tetradecanoate **13a** (12.0 g,32.0 mmol, 89%).

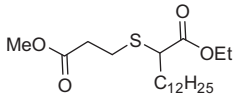

Chemical Formula: $C_{20}H_{38}O_4S$
Exact Mass: 374.2491
13a

^{1}H NMR ($CDCl_3$) δ 4.14–4.25 (m, 2H), 3.69 (s, 3H), 3.20–3.26 (m, 1H), 2.81–2.92 (m, 2H), 2.56–2.64 (m, 2H), 1.81–1.92 (m, 2H), 1.60–1.68 (m, 2H), 1.21–1.48 (m, 21H), 0.87 (t, J = 6.8 Hz, 3H); ^{13}C NMR ($CDCl_3$) δ 172.7 (s), 172.1 (s), 61.1 (s), 51.7 (s), 46.8 (s), 34.4 (s), 31.9 (s), 31.4 (s), 29.2–29.6 (m), 27.3 (s), 26.2 (s), 22.7 (s), 14.2 (s), 14.1 (s); MS (ESI) *m*/*z* 375.4 (M^++1).

A similar procedure was followed with the shorter bromo ester **12** to give ethyl 2-(3-methoxy-3-oxopropylthio)octanoate **13b** (3.51 g, 12.1 mmol, 93%).

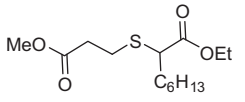

Chemical Formula: $C_{14}H_{26}O_4S$
Exact Mass: 290.1552
13b

^{1}H NMR ($CDCl_3$) δ 4.14–4.25 (m, 2H), 3.69 (s, 3H), 3.20–3.26 (m, 1H), 2.80–2.92 (m, 2H), 2.56–2.64 (m, 2H), 1.81–1.92 (m, 2H), 1.60–1.68 (m, 2H), 1.21–1.48 (m, 9H), 0.87 (t, J = 6.8 Hz, 3H); ^{13}C NMR ($CDCl_3$) δ 172.7 (s), 172.0 (s), 61.1 (s), 51.7 (s), 46.8 (s), 34.4 (s), 31.5 (s), 31.3 (s), 28.8 (s), 27.3 (s), 26.2 (s), 22.5 (s), 14.2 (s), 14.0 (s); MS (ESI) *m*/*z* 291.3 (M^++1).

As for the two long chain analogs, the bis primary alcohols were prepared, in this case by reducing both esters simultaneously. Thus, to an ice-cooled solution of 3.8 g (13.1 mmol, 1 equiv) of **13a** in 100 mL of THF was added 2.0 g (52.6 mmol, 4.0 equiv) of lithium aluminum hydride. Then the reaction mixture was stirred at 0 °C for 10 min. Then the reaction temperature was raised to 60 °C overnight, then cooled down to rt. The resulting mixture was filtered, and concentrated before 100 mL ethyl acetate was added. The organic layer was washed with 1 N HCl, saturated $NaHCO_3$ solution, followed by a saturated NaCl solution. Solvent was removed at reduced pressure and the crude mixture was purified on silica column (ethyl acetate–hexanes, 25–50%) to give the product 2-(3-hydroxypropylthio)tetradecan-1-ol **14a** (2.6 g, 11.8 mmol, 90%).

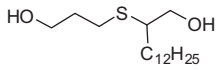

Chemical Formula: $C_{17}H_{36}O_2S$
Exact Mass: 304.2436
14a

^{1}H NMR ($CDCl_3$) δ 3.76 (t, J = 6.0 Hz, 2H), 3.55–3.60 (m, 1H), 3.46–3.52 (m, 1H), 2.58–2.76 (m, 3H), 2.00 (s, 2H), 1.81–1.89 (m, 2H), 1.45–1.62 (m, 3H), 1.21–1.44 (m, 19H), 0.88 (t, J = 6.8 Hz, 3H); ^{13}C NMR ($CDCl_3$) δ 63.9 (s), 61.5 (s), 49.6 (s), 32.4 (s), 31.9 (s), 31.8 (s), 29.3–29.6 (m), 27.1 (s), 26.7 (s), 22.7 (s), 14.1 (s); MS (ESI) *m*/*z* 327.3 ($M+Na^+$).

A similar procedure was followed to reduce **13b** to give 2-(3-hydroxypropylthio)octan-1-ol **14b** (1.87 g, 8.51 mmol, 88%).

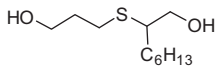

Chemical Formula: $C_{11}H_{24}O_2S$
Exact Mass: 220.1497
14b

^{1}H NMR ($CDCl_3$) δ 3.76 (t, J = 6.0 Hz, 2H), 3.46–3.52 (m, 1H), 2.58–2.76 (m, 3H), 2.03 (s, 2H), 1.81–1.89 (m, 2H), 1.45–1.62 (m, 3H), 1.21–1.44 (m, 8H), 0.88 (t, J = 6.8 Hz, 3H); ^{13}C NMR ($CDCl_3$) δ 63.9 (s), 61.5 (s), 49.6 (s), 32.4 (s), 31.8 (s), 31.7 (s), 29.1 (s), 27.1 (s), 26.7 (s), 22.6 (s), 14.0 (s); MS (ESI) *m*/*z* 203.3 (M^+−OH).

The corresponding sulfide **14a** (10.6 g, 34.8 mmol, 1 equiv) was dissolved in CH_2Cl_2 (180 ml) and *m*-CPBA (15.0 g, 87.0 mmol, 2.5 equiv) was added to it at 0 °C (ice bath). The reaction mixture was allowed warm to rt and stirred for 8 h at rt. Volatiles were evaporated under reduced pressure. The residue was taken up in ethyl acetate (150 mL) and washed with 10% Na_2SO_3, saturated $NaHCO_3$, and brine. The organic layer was then dried over anhydrous Na_2SO_4. The volatiles were evaporated under reduced pressure to yield the crude mixture that was purified on silica column (ethyl acetate–hexanes, 30–80%) to yield the pure product 2-(3-hydroxypropylsulfonyl)tetradecan-1-ol **15a**. (9.0 g, 26.8 mmol, 77%).

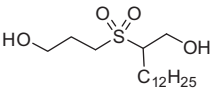

Chemical Formula: $C_{17}H_{36}O_4S$
Exact Mass: 336.2334
15a

^{1}H NMR ($CDCl_3$) δ 3.90–4.05 (m, 2H), 3.79 (t, J = 6.0 Hz, 2H), 3.22 (t, J = 7.6 Hz, 2H), 2.94–3.02 (m, 1H), 2.49 (s, 2H), 2.06–2.15 (m, 2H), 1.84–1.95 (m, 1H), 1.52–1.72 (m, 1H), 1.45–1.55 (m, 1H), 1.22–1.40 (m, 19H), 0.88 (t, J = 6.8 Hz, 3H); ^{13}C NMR ($CDCl_3$) δ 64.6 (s), 60.6 (s), 59.6 (s), 49.4 (s), 31.4 (s), 29.3–2.6 (m), 26.9 (s), 24.3 (s), 24.2 (s), 22.5 (s), 14.0 (s); MS (ESI) *m*/*z* 337.3 (M^++H).

Sulfide **14b** was oxidized as described above for sulfide **14a** to give methyl 2-(3-hydroxypropylsulfonyl)octan-1-ol **15b** (1.79 g, 7.1 mmol, 81%).

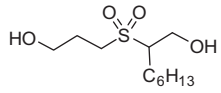

Chemical Formula: $C_{11}H_{24}O_4S$
Exact Mass: 252.1395
15b

^{1}H NMR ($CDCl_3$) δ 3.90–4.05 (m, 2H), 3.75 (t, J = 6.0 Hz, 2H), 3.21 (t, J = 7.6 Hz, 2H), 2.94–3.02 (m, 1H), 2.82 (s, 2H), 2.03–2.11 (m, 2H), 1.84–1.95 (m, 1H), 1.58–1.69 (m, 1H), 1.42–1.52 (m, 1H), 1.22–1.40 (m, 7H), 0.86 (t, J = 6.8 Hz, 3H); ^{13}C NMR ($CDCl_3$) δ 64.6 (s), 60.6 (s), 59.6 (s), 49.4 (s), 31.4 (s), 29.0 (s), 26.9 (s), 24.3 (s), 24.2 (s), 22.5 (s), 14.0 (s); MS (ESI) m/z 253.3 (M^++H).

As above, the vinyl sulfones were formed and primary iodide introduced in a two-step protocol. Thus, to a solution of 2.0 g (7.92 mmol, 1 equiv) of **15b** and diisopropyl ethylamine (5.1 g, 39.4 mmol, 5 equiv) in 40 mL of CH_2Cl_2 was added mesyl chloride (2.74 g, 19.0 mmol, 2.4 equiv). Then the reaction mixture was stirred at rt for 2 h. The mixture was filtered, and the filtrate was washed with saturated $NaHCO_3$ solution and then dried over sodium sulfate. The organic solvent was concentrated. The residue was dissolved into acetone (30 mL) followed by NaI (3.6 g, 16 mmol, 3 equiv) and $NaHCO_3$ (1.0 g, 11.9 mmol, 2.2 equiv). The reaction mixture was stirred at rt overnight, filtered, and concentrated. Then, 50 mL water and 50 mL ethyl acetate were added to the residue, and the organic layer was collected and the aqueous layer was re-extracted twice with ethyl acetate. The combined organics were dried over sodium sulfate and then removed at reduced pressure. Next, 100 mL ethyl acetate was added followed by diisopropylethylamine (5 mL). The reaction mixture was stirred at room temperature for 3 days. The organic solvent was removed at reduced pressure and the crude mixture was purified on silica column (ethyl acetate–hexanes, 0–15%) to give the product 2-(3-iodopropylsulfonyl)oct-1-ene **16b** (2.23 g, 6.49 mmol, 82%).

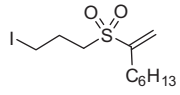

Chemical Formula: $C_{11}H_{21}IO_2S$
Exact Mass: 344.0307
16b

^{1}H NMR ($CDCl_3$) δ 6.25 (s, 1H), 5.83 (s, 1H), 3.28 (t, J = 6.8 Hz, 2H), 3.08 (t, J = 7.6 Hz, 2H), 2.41 (t, J = 7.6 Hz, 2H), 2.21–2.30 (m, 2H), 1.52–1.63 (m, 2H), 1.25–1.42 (m, 6H), 0.89 (t, J = 6.8 Hz, 3H); ^{13}C NMR ($CDCl_3$) δ 145.9 (s), 122.0 (s), 49.7 (s), 28.3 (s), 26.6 (s), 25.6 (s), 24.6 (s), 23.1 (s), 19.4 (s), 10.9 (s); MS (ESI) m/z 367.2 (M+Na^+).

A similar procedure was followed to convert **15a** to 2-(3-iodopropylsulfonyl)tetradec-1-ene **16a** (346 mg, 0.81 mmol, 69%).

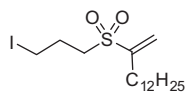

Chemical Formula: $C_{17}H_{33}IO_2S$
Exact Mass: 428.1246
16a

^{1}H NMR ($CDCl_3$) δ 6.23 (s, 1H), 5.81 (s, 1H), 3.28 (t, J = 6.4 Hz, 2H), 3.07 (t, J = 7.6 Hz, 2H), 2.40 (t, J = 7.6 Hz, 2H), 2.21–2.30 (m, 2H), 1.52–1.63 (m, 2H), 1.25–1.42 (m, 18H), 0.87 (t, J = 6.8 Hz, 3H); ^{13}C NMR ($CDCl_3$) δ 145.9 (s), 122.0 (s), 49.7 (s), 28.7 (s), 26.1–26.6 (m), 25.9 (s), 24.6 (s), 23.0 (s), 19.5 (s), 11.0 (s); MS (ESI) m/z 451.3 (M+Na^+).

A procedure similar to that described above for CVS-18 was used to obtain *N*,*N*,*N*-trimethyl-3-(tetradec-1-en-2-ylsulfonyl) propan-1-aminium chloride CVS-12 (**17a**, 23 mg, 0.058 mmol, 58%).

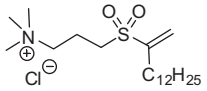

Chemical Formula: $C_{20}H_{42}ClNO_2S$
Exact Mass: 395.2625
17a

^{1}H NMR (CD_3OD) δ 6.25 (s, 1H), 5.98 (s, 1H), 3.48–3.56 (m, 2H), 3.27 (s, 2H), 3.16–3.22 (m, 11H), 2.45 (t, J = 7.6 Hz, 2H), 2.20–2.28 (m, 2H), 1.60–1.66 (m, 2H), 1.26–1.44 (m, 16H), 0.90 (t, J = 6.8 Hz, 3H); ^{13}C NMR (CD_3OD) δ 149.2 (s), 125.1 (s), 64.3 (s), 52.2 (m), 31.4 (s), 28.8–29.3 (m), 27.7 (s), 26.7 (s), 22.3 (s), 16.2 (s), 13.0 (s); MS (ESI) m/z 360.3 (M^+).

A procedure similar to that described above for CVS-18 was used to provide *N*,*N*,*N*-trimethyl-3-(oct-1-en-2-ylsulfonyl)propan-1-aminium chloride CVS-6 (**17b**, 11 mg, 0.035 mmol, 72%).

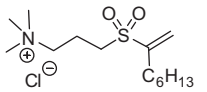

Chemical Formula: $C_{14}H_{30}ClNO_2S$
Exact Mass: 311.1686
17b

^{1}H NMR ($CDCl_3$) δ 6.28 (s, 1H), 5.88 (s, 1H), 4.05–4.13 (m, 2H), 3.43 (s, 9H), 3.22 (t, J = 6.8 Hz, 2H), 2.38–2.46 (m, 4H), 1.55–1.65 (m, 2H), 1.28–1.42 (m, 6H), 0.89 (t, J = 6.8 Hz, 3H); ^{13}C NMR ($CDCl_3$) δ 149.1 (s), 125.8 (s), 54.1 (s), 48.3 (s), 31.5 (s), 29.6 (s), 28.6 (s), 27.7 (s), 22.5 (s), 16.6 (s), 14.0 (s); MS (ESI) m/z 276.4 (M^+).

2.3. ATX assay

ATX inhibition was performed using an ATX Inhibitor Screening Kit (K-4200, Echelon Biosciences, Inc. Salt Lake City, UT). Stock solutions (1 mM) of each compound were made in DMSO and then diluted with water to the appropriate experimental concentration. Fourteen final inhibitor concentrations from 0.1 to 10,000 nM were employed to calculate K_i values. DMSO was spiked into each reaction mixture to equalize vehicle concentrations. The assay employs the fluorescence-quenched, ATX analog FS-3 as the ATX substrate[25] and recombinant, human ATX purified from Sf9 insect cells as the enzyme source. Compounds were pre-incubated with the enzyme at 25 °C for 10 min, after which FS-3 was added. The rate of fluorescence increase was measured between 5 and 25 min after substrate addition. In all circumstances fluorescence increase was linear during this time window. Rates were normalized to control reactions that contained all reaction components except the test compound.

2.4. Dilution/dialysis for reaction of 10b (CVS-16) or 21 (PVS-16) with ATX

ATX was incubated with compound **10b** or **21** (0, 1 or 10 μM) for two minutes in 50 mM Tris–Cl pH 8.0, 5 mM KCl, 1 mM $CaCl_2$, 1 mM $MgCl_2$, 140 mM NaCl, 1 mg/ml Fatty Acid Free BSA. Half of each reaction was placed in a centrifugal filtration device (Millipore) with a molecular weight cutoff of 30 kDa and subjected to repeated rounds of concentration and dilution using buffer absent of test compound. ATX activity was then assessed in each sample by monitoring FS-3 (1 μM) fluorescence increase over time and compared to the activity of ATX not incubated with test compound or subjected to dialysis.

2.5. Cell culture

Cell lines were acquired from the American Type Culture Collection or ATCC (Manassas, VA). Human cancer cell lines SKOV-3, OVCAR-3, PC-3 and MDA-MB-231 cells were maintained in RPMI (Mediatech Inc., Manassas, VA) supplemented with 10% fetal bovine serum or FBS (Sigma). MeWo fibroblast malignant melanoma cells were cultured similarly, but supplemented with only 5% FBS. HT-29 human colon cancer cells and SB-2 human non-metastatic melanoma cells were maintained in DMEM (Mediatech) supplemented with 10% FBS.

2.6. Cell viability assay

Approximately 5000 cells were grown in each well of a 96-well plate for 24 h prior to the addition of CVS-16 (**10b**) compound at the indicated concentrations for 48 h. The assay was then performed by removing medium from the 96-well plate and replacing it with serum free media containing CellTiter-Blue® reagent (Promega Corporation, Madison, WI) and incubating for 4–6 h at 37 °C. Then the fluorescent absorbance was measured with a microplate reader, the SpectraMax M2 model (Molecular Devices, Sunnyvale, CA).

2.7. Wound healing assay

Cells were seeded in triplicates in 24-well plates and then grown to confluence. 'Wounds' were then created using a pipette tip. The wells were then repeatedly rinsed using serum-free medium followed by the addition of 18:1 LPA (Avanti Polar Lipids, Alabaster, AL) or CVS-16 (**10b**) to the wells and incubated for 24 h. Photomicrographs were taken of the wells, at least six per well, and treatments were performed in triplicate. The distance between confluent monolayers was measured.

2.8. Animal model of melanoma

Six-week old female athymic nude mice acclimated to the animal facility for one week prior to the study commencement. Animals were anesthetized before tumor cell injection into their right flank with Glycosan Extracel® (BioTime, Inc, Alameda, CA) containing approximately 1×10^6 MeWo cells per 0.15 mL injection. Extracel® was used in this study over traditional Matrigel to eliminate potential interference of exogenous mouse growth factors which could have affected our in vivo study. In addition, Glycosan Extracel® allows us to conserve resources through the achievement of a 100% tumor efficiency rate, whereby this rate is typically unachievable otherwise. Injected mice were measured for tumor formation, tumor volume, body weight and body conditioning scores. After 3 weeks, 100% of mice displayed tumor formation at which time they were randomized into treatment groups; PBS control ($n = 10$), CVS-16 (**10b**) at 20 mg/kg ($n = 5$) or 50 mg/kg ($n = 5$), DMF control ($n = 10$), HA-130 at 30 mg/kg ($n = 5$) and PF-8380 at 30 mg/kg ($n = 5$) dose per 0.1 mL injection. Mice in each treatment group were anesthetized (2–4% isoflurane) before i.p. treatment injections three times a week over the course of the 65-day study. The animals were euthanized according to the animal use protocol approved by the University of Georgia IACUC committee. The tumor volume (mm^3) was calculated using the equation: tumor volume = $(\text{width})^2 \times \text{length}/2$, and then graphed using GraphPad Prism (La Jolla, CA). The tumor volume for each group and overall significance was plotted.

2.9. Tumor specimen analysis

Melanoma tumors were dissected from the right flank of athymic nude mice and flash-frozen with cryomatrix (Thermo Fisher Scientific Inc, Waltham, MA) in 2-methylbutane (Sigma) and cooled to −140 °C. Cryopreserved tumors were cut in 9 μm sections using a cryostat (Thermo Fisher Scientific) and then mounted on microscope slides. Hematoxylin and eosin staining was performed according to standard protocols and processed for pathological evaluation.

For tissues stained with antibodies specific for immunofluorescence, tissue sections were first blocked for 30 min in 5% donkey serum (Jackson ImmunoResearch Laboratories Inc, West Grove, PA) diluted in phosphate-buffered saline (PBS) for 30 min at room temperature. The tumor sections were then incubated in primary antibodies at 4 °C overnight using a humidity chamber. The following day slides were washed with PBS and the primary antibody was detected using a fluorescent secondary antibody. After washing the slides again with PBS, they were mounted with Permount (Thermo Fisher Scientific) and imaged using an X71 inverted microscope (Olympus, Center Valley, PA) at 20× magnification. Overlapping pictures were aligned to generate an image of an entire tumor cryosection. The tumor area was automatically calculated using the polygon tool in Image-Pro Precision software (Media Cybernetics, Inc., Rockville, MD), then the Ki-67 pixel intensity was automatically determined. The average pixel staining intensity per area measurement was plotted.

2.10. Serum analysis

Whole blood was collected from animals at necropsy and placed into a Becton Dickinson Microtainer® tube with serum separator additive and allowed to clot for at least 20 min in a vertical position at room temperature. The tubes were then inverted five times prior to centrifugation at 2000 RCF for 10 min at room temperature. The serum was transferred to a glass vial and stored in −80 °C until use. Approximately 200 μl of serum was obtained from each mouse. From that, 100 μl of serum was analyzed for cytokines, chemokines, growth factors and interleukins using the mouse Bio-Plex, 23-Plex panel (Bio-Rad, Hercules, CA) and following the instructions provided by the manufacturer. The assay plates were measured using the Bio-Plex Multiplex Suspension Array system (Bio-Rad). Serum samples were measured via comparison to an 8-point standard dilution series included as an integral component of the high-throughput assay. For analysis of ATX, the remaining 100 μl of serum was processed using the mouse ectonucleotide pyrophosphatase/phosphodiesterase family member 2 (ENPP2) ELISA kit according to the instructions provided by the manufacturer (MyBioSource.com, San Diego, CA).

2.11. Statistics

The statistical differences were analyzed using an analysis of variance (ANOVA) test, followed by Bonferroni's multiple comparison test between groups using GraphPad Prism. When comparing only two groups, the Student's *t*-test was used. Where it is indicated in the figures, $^{*}p<0.05$, $^{**}p<0.01$ and $^{***}p<0.001$ indicate the levels of significance.

3. Results

3.1. Chemical synthesis of vinyl sulfone analogs

Although palladium or copper-promoted reaction of sulfinic acids with alkyl halides or triflates can provide vinyl sulfones in

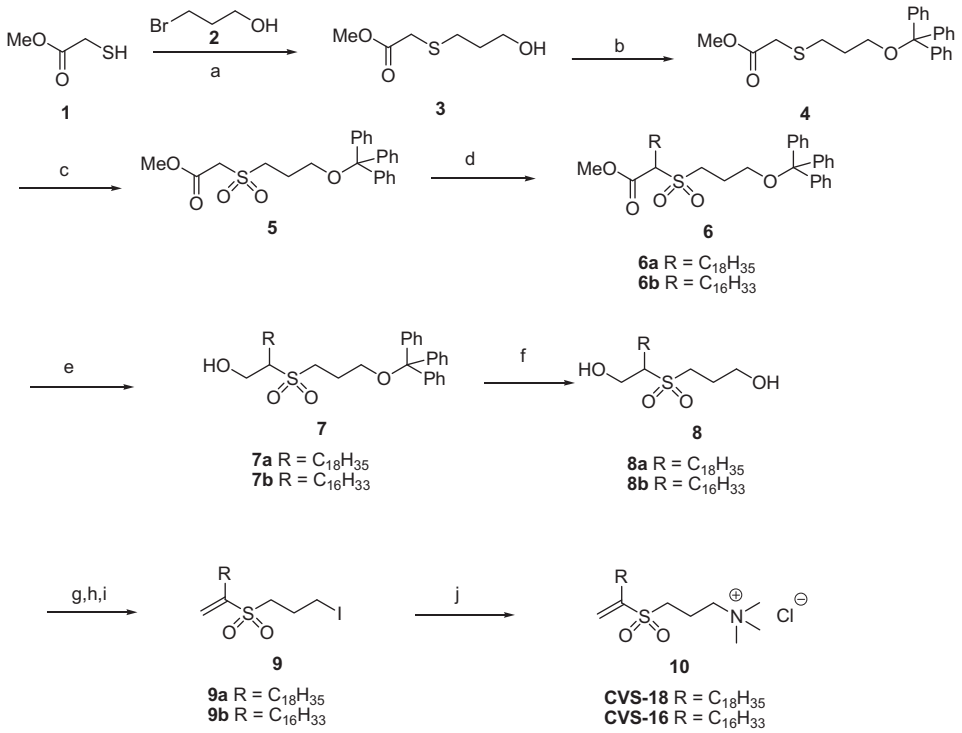

Figure 1. Synthesis of quaternary ammonium vinyl sulfone analogs **10** (CVS-18, CVS-16). Reagents and conditions: (a) K_2CO_3, acetone, reflux, 2 h, 98%; (b) TrCl, triethylamine, dichloromethane, 94%; (c) *m*CPBA, dichloromethane, 0 °C to room temperature, 8 h, 95%; (d) NaH, RI, DMF, 72–88%; (e) $LiAlH_4$, diethyl ether, at 0 °C, 10 min, 34–51%; (f) TFA, dichloromethane, 2 h, 66–81%; (g) MsCl, DIPEA, dichloromethane; (h) NaI, acetone; (i) DIPEA, EtOAc, 45–81% for three steps; (j) trimethylamine in EtOH, dichloromethane, 4 days, 71–85%.

good yield,[26] the harsh conditions (80 °C) were not appropriate for these analogs. Our strategy for the synthesis of desired targets involves conversion of the key intermediate β-hydroxy sulfones **8** to vinyl sulfones **9**. In addition, the quaternary ammonium salts **10** and **17** were prepared in the final step to avoid difficulties in purification of reactive electrophilic species.

Two different synthetic routes were carried out, based on the availability of the starting materials. The vinyl sulfone analogs with the 16:0 and 18:1 alkyl chains were prepared as shown in Fig. 1. We selected these chain lengths based on the known bioactivity of LPA agonists for the LPARs, with the expectation that these would be the best probes for the ATX active site. The formation of the thioether **3** could be performed by displacement of the bromide anion **1** with bromide in good yield (98%). The primary hydroxyl group was then tritylated (TrCl, Et_3N) to give compound **4**. Conversion of sulfide **4** to sulfone **5** was accomplished by oxidation with *m*-CPBA in dichloromethane. In order to alkylate compound **5** regioselectively, we chose sodium hydride as the base so that the reaction could be performed at room temperature in moderate yield; the regioisomer was not detected.

Next, the reduction of ester and removal of the trityl group was carried out to give the diol **8**. However, preliminary attempts to reduce the ester were unsuccessful. An unexpected over-reduction of hydroxyl to methyl was observed using either excess lithium aluminum hydride or sodium borohydride. Possible reasons for the over-reduction include excess reductant, long reaction time, reaction temperature, or the proximity of the β-sulfone moiety, but this was not further explored. After optimization, moderate yields of reduction (34–51%) could be obtained by using 1 equiv of lithium aluminum hydride in THF at 0 °C for 10 min. The conversion of diols **8** to vinyl sulfone **9** involved a three-step sequence, although no intermediates need to be isolated. Conversion of **8** to the corresponding mesylate and subsequent iodination afforded the iodo intermediates. Next, the β-iodo sulfones were β-dehydroiodinated by treatment with diisopropylethylamine (DIPEA) in EtOAc to give the desired vinyl sulfones. Importantly, γ-iodoalkyl groups were stable in the presence of DIPEA, which allowed us to install the quaternary ammonium derivative in a subsequent step. Thus, the corresponding quaternary ammonium salts could be obtained by treating the remaining iodoalkyl group with trimethylamine in a mixture of ethanol and dichloromethane for 4 days. Recrystallization of crude salts from CH_3OH–Et_2O provided the final targets **10** (CVS-18 and CVS-16) as white solids (Fig. 1).

In an effort to synthesize the shorter chain vinyl sulfone, which we hypothesized would be more water-soluble and still retain ATX inhibitory activity, we took the advantage of commercially available α-bromo esters **12**, which reacted with thiol directly to give the corresponding sulfide (Fig. 2). Excess lithium aluminum hydride was employed to reduce ester groups to diols **14**. Oxidation with *m*-CPBA in dichloromethane at 0 °C converted the sulfides **14a**,**b** to sulfones **15a**,**b** in good yield. Then final targets **17a** and **17b** (CVS-6 and CVS-12) were prepared from sulfones **15a**,**b** in an analogous fashion described previously for the structurally-similar analog **10a** (Fig. 2).

A non-choline-like head vinyl sulfone **21** (PVS-16) that retained the 16:0 alkyl chain was synthesized as a negative control. Alkylation of the commercially available compound **18** using sodium hydride (60% in mineral oil) as base proceeded in high yield (95%). After the hydrophobic chain was installed, phenyl vinyl sulfone compound **21** could be achieved by mesylation/iodination and elimination as employed above (Fig. 3).

3.2. Kinetic inhibition of ATX

The analysis of the kinetic inhibition of ATX demonstrated that the enzymatic activity decreased in a time-dependent manner.

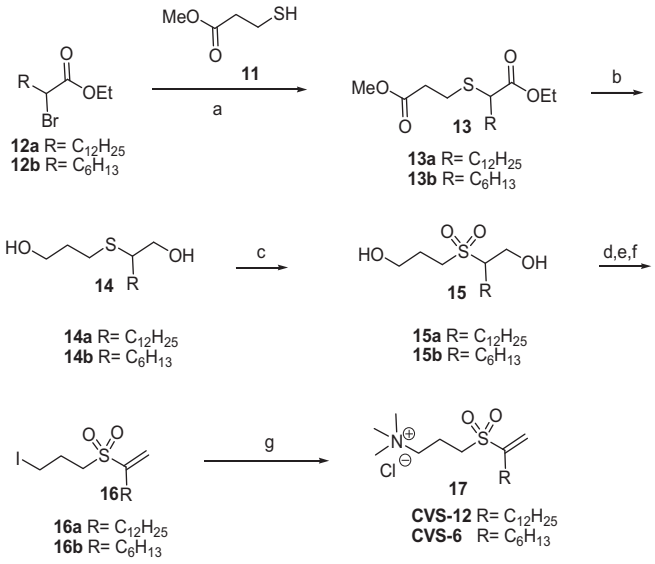

Figure 2. Synthesis of quaternary ammonium vinyl sulfone analogs **17** (CVS-12, CVS-6). Reagents and conditions: (a) K_2CO_3, acetone, reflux, 2 h, 89–93%; (b) $LiAlH_4$, THF, at 60 °C, overnight, 88–90%; (c) *m*-CPBA, dichloromethane, 0 °C to room temperature, 8 h, 77–81%; (d) MsCl, DIPEA, dichloromethane; (e) NaI, acetone; (f) DIPEA, EtOAc, 69–82% for three steps; (g) trimethylamine in EtOH, dichloromethane, 4 days, 58–72%.

However, the time course of inhibition is very rapid since pre-incubating ATX with the compound CVS-16 (**10b**) for just 2 min results in complete inhibition. Different hydrophobic chain lengths were synthesized to study the structure–activity relationship of the compound. The inhibition of ATX by the vinyl sulfone ATX analogs CVS-18 (**10a**) and CVS-16 (**10b**) was tested using an ATX inhibitor screening kit (Echelon Biosciences, Inc.) in a dose-response mode (Table 1). ATX activity was measured by the hydrolysis of the fluorogenic ATX analog FS-3, which has a K_M value of 6.3 μM.[25] The results showed that all analogs except the shorter-chain analog CVS-6 (**17b**) inhibited ATX effectively, with C18:1 ATX showing the greatest inhibition.[27] Non-quaternary ammonium head group vinyl sulfone PVS-16 (**21**) showed no inhibitory effect at the highest test concentration, which reveals the importance of quaternary ammonium head group for achieving the binding affinity (Table 1).

We tested the irreversible nature of compound CVS-16 (**10b**) by performing a washout experiment (Supplementary Fig. 1). ATX was pre-incubated with compound CVS-16 (**10b**) or buffer for two minutes, after which time half of each reaction mixture was placed in a centrifugal filtration device. Over approximately one hour, samples were subjected to multiple rounds of concentration and dilution, resulting in over 1000-fold dilution of compounds CVS-16 (**10b**) and PVS-16 (**21**). ATX activity was then assessed by monitoring FS-3 hydrolysis. Attempted wash out of CVS-16 (**10b**) did not decrease the ATX inhibition, a finding consistent with CVS-16 (**10b**) irreversibly binding to the enzyme. PVS-16 showed no evidence of inhibiting ATX activity whether or not the compound was subjected to the washout experiment.

Table 1
Inhibition of ATX phosphodiesterase activity by vinyl sulfone analogs

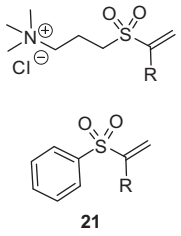

Compound	R	K_i (μM)	95% CI
10a (CVS-18)	$C_{18}H_{35}$	2.43	2.08–2.77
10b (CVS-16)	$C_{16}H_{33}$	3.50	3.21–3.8
17a (CVS-12)	$C_{12}H_{25}$	1.79	1.64–1.93
17b (CVS-6)	C_6H_{13}	NE[a]	NA
21 (PVS-16)	$C_{16}H_{33}$	NE[a]	NA

[a] NE, no effect was shown at the highest concentration (10 μM) tested.

3.3. In vitro biological activity

In order to determine whether CVS-16 (**10b**) possessed in vitro biological activity, studies were conducted to explore the functional potency of CVS-16 (**10b**) against cell viability. For these studies, we used multiple cancer cell lines to represent a wide range of subtypes including HT-29 (colon), PC-3 (prostate), MDA-MB-231 (breast), MeWo (melanoma), SB-2 (melanoma), OVCAR-3 (ovarian) and SKOV-3 (ovarian). In all cell lines, the CVS-16 (**10b**) compound reduced cell viability to some extent (Fig. 4A) with significant activity of CVS-16 (**10b**) observed between 0.5 and 5 μM (Fig. 4B). The IC_{50} values of CVS-16 (**10b**) are listed in Table 2 and the IC_{50} values of PVS-16 are in Supplementary Figure 2. Interestingly, CVS-16 (**10b**) had strong activity against MDA-MB-231 cells (IC_{50} = 0.39 μM) in comparison to the other cell types, but it was effective against all cell lines tested ($^*p$>0.05). As a control, we also examined the effect of PVS-16 (**21**) cell against viability and observed that most cell types were unaffected by its presence (Fig. 4C), especially at relevant concentrations (Fig. 4D).

Next we assessed confluent monolayer wounding and measured subsequent closure using MDA-MB-231, OVCAR-3, SKOV-3 and MeWo cells in the presence or absence of LPA (18:1, 1 μM) and/or CVS-16 (**10b**, 5 μM). For all cell lines examined, we observed that CVS-16 (**10b**) significantly ($^*p$<0.05 vs untreated) inhibited wound healing, which encompasses cell proliferation

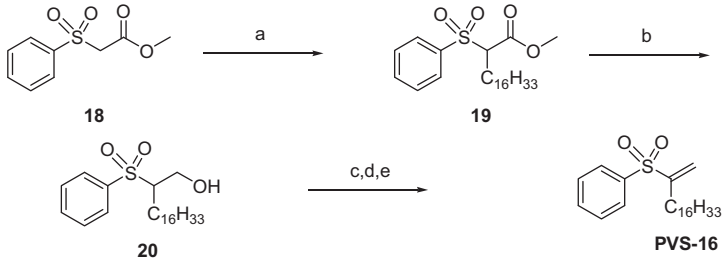

Figure 3. Synthesis of non-quaternary ammonium vinyl sulfone **21** (PVS-16). Reagents and conditions: (a) NaH, $C_{16}H_{33}I$, DMF, 95%; (b) $LiAlH_4$, Diethyl ether, −78 °C, 15 min, 33%; (c) MsCl, DIPEA, dichloromethane; (d) NaI, acetone; (e) NaOtBu, EtOAc/DCM, 77% for three steps.

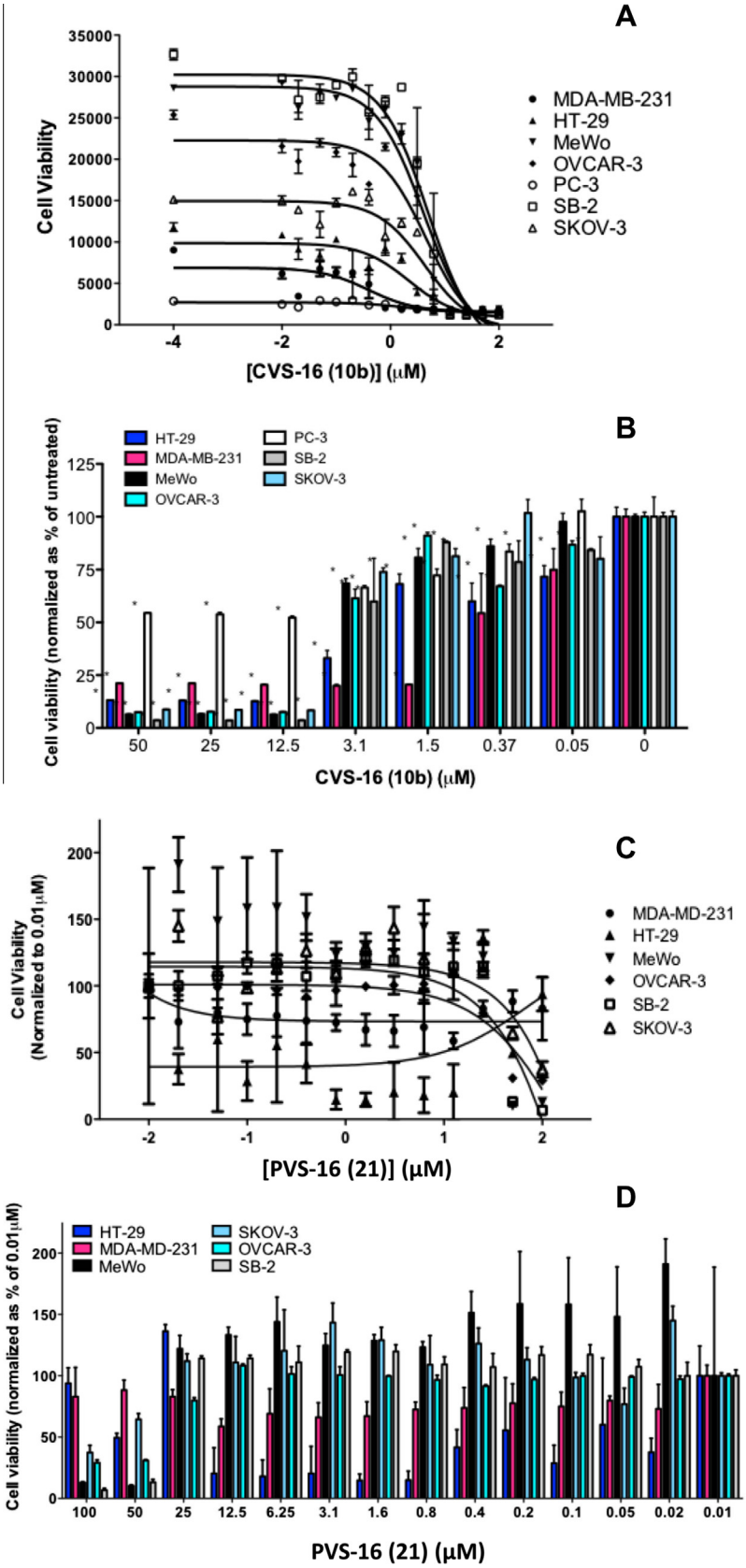

Figure 4. CVS-16 (**10b**) reduces cell viability in multiple cancer cell lines. Cell viability was measured using CellTiter® Blue after treating cells with the indicated concentration of CVS-16 (**10b**) for 48 h. The data is presented as a viability curve (A) and bar graph (B). $^{*}p<0.05$ comparing 0 μM to CVS-16-treated condition for each cell line using the student's *t*-test. The negative control, PVS-16 (**21**), a phenyl vinyl sulfone compound was used against multiple cancer cell lines. The data is presented as a viability curve (C) and bar graph (D).

Table 2
Inhibition of **10b** (CVS-16) in various cell lines

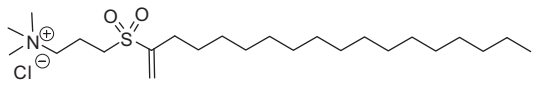

10b

Cell line	Average IC_{50} (μM)	95% CI
PC-3	1.93	0.91–4.45
OVCAR-3	4.44	2.53–8.10
HT-29	2.11	0.97–4.88
MeWo	4.08	2.87–5.79
MDA-MB-231	0.39	0.14–1.04
SB-2	4.89	2.73–9.12
SKOV-3	6.74	2.55–7.22

and migration from a denuded front that eventually closes the gap between confluent cell monolayers on either side (Supplementary Fig. 3). In addition, the CVS-16 (**10b**) analog (5 μM) displays a signification reduction (over 75%) in both OVCAR-3 and MDA-MB-231 cell lines. Unexpectedly in most cases, LPA was not able to overcome the inhibition of CVS-16 (**10b**) on wound closure when these two reagents were combined.

Since the in vitro data thus far suggested that CVS-16 (**10b**) has a significant impact against MeWo cells, we wanted to compare the functional activity of this compound against other state-of-the-art ATX inhibitors; for this comparison, we selected: HA-130[15a] and PF-8380.[15b] Since melanoma cells are notoriously and intrinsically resistant to traditional chemotherapy, we also included several negative controls: dacarbazine (DTIC), paclitaxel (PTX/TAX), vincristine (VCR) and cisplatin (CDDP). Indeed, the chemotherapy had little impact on MeWo cells—never dropping below 50% cell viability (Fig. 5). In contrast, the ATX inhibitors CVS-16 (**10b**) and HA-130 were able to reduce cell viability below 25%. Although there was no significant difference in activity between HA-130 with either of the other ATX inhibitors, CVS-16 (**10b**) was significantly different from PF-8380 ($^{*}p<0.05$) and chemotherapy ($^{**}p<0.01$).

3.4. Inhibition of melanoma progression and angiogenesis

In light of the fact that the data thus far suggested CVS-16 (**10b**) had significant biological activity in vitro, we wanted to next assess

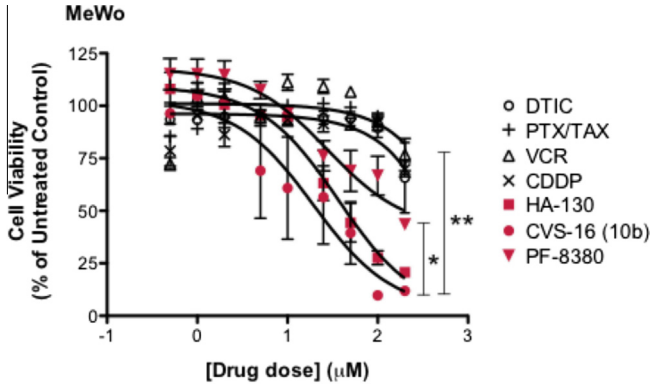

Figure 5. ATX inhibitors reduce the cell viability of MeWo melanoma cells, in contrast with chemotherapy. Cell viability was measured using CellTiter® Blue after treating cells with the indicated concentration of: CVS-16 (**10b**), HA-130, PF-8380, dacarbazine (DTIC), paclitaxel (PTX/TAX), vincristine (VCR) and cisplatin (CDDP) for 48 h. $^{*}p<0.05$ comparing CVS-16 (**10b**) to PF-8380-treated cells or $^{**}p<0.01$ comparing CVS-16 (**10b**) to chemotherapy (DTIC, PTX/TAX, VCR and CDDP) using the student's *t*-test.

whether it also had in vivo activity. Since there is a dearth of clinical therapeutics to treat melanomas lacking BRAF mutations, we examined CVS-16 (**10b**) in an animal model of melanoma. After establishing small pigmented melanoma tumors using MeWo cells injected with Glycosan Extracel®, the mice were randomized into groups and then treated every-other-day with either diluent (control), CVS-16 (**10b**) at 20 mg/kg or CVS-16 (**10b**) at 50 mg/kg, which began 21 days post tumor cell injection. Prior to day 45, the tumor sizes in all groups appeared identical, but then began to diverge with the control groups displaying a linear rate of growth (Fig. 6A). The group of mice treated with 20 mg/kg of CVS-16 (**10b**) also showed linear growth around day 50. On day 57, the tumor sizes between groups achieved statistical significance (Fig. 6B, $^{*}p<0.05$, 50–40 mg/kg CVS-16 (**10b**) vs control; day 65—$^{***}p<0.001$, 50–40 mg/kg CVS-16 (**10b**) vs control) and this trend continued through the conclusion of the study, whereby control groups reached maximum allowable tumor volume. Mouse weight data was also collected (Supplementary Fig. 4).

Of note is that on the 46th day of the study, the group of mice treated with 50 mg/kg of CVS-16 (**10b**) looked severely dehydrated and required medical intervention. Unfortunately, one mouse in the 50 mg/kg group (with a very small tumor and no signs of ascites upon necropsy) rapidly declined in health and then died the following day, even after veterinarians helped treat the mouse for this condition. Thus, on the 48th day, we reduced the concentration of CVS-16 (**10b**) to 40 mg/kg (marked with an arrow) so that the experiment could continue without additional mice succumbing to a possible unspecified side effects of CVS-16 (**10b**) at 50 mg/kg. Subsequently, all of the mice in this group were then fed a special diet to curb dehydration, in addition to their regular chew pellets and no others died before the date of necropsy.

Upon necropsy, we collected tissues and serum from all mice remaining in the study. We then measured the mouse serum for 25 different secreted factors, including cytokines, chemokines, interleukins, etc. Understanding that many interleukins would only be expressed by animals with immune-intact systems, we also coupled this study to another whereby we treated C57/Bl6 animals (n=20) with CVS-16 (**10b**) and measured their serum (data not shown). Interestingly, the most significant decrease in chemokines among treated animal serum from the present study shown herein was the keratinocyte chemoattractant (KC, also referred to as Chemokine C-X-C Motif Ligand 1 (CXCL1) or the Melanoma Growth Stimulating Activity Alpha protein) (Fig. 6C, $^{*}p<0.05$, $^{***}p<0.001$). The KC/CXCL-1 chemokine is homologous to the human growth regulated oncogene alpha (GRO-alpha), which is regulated by ATX[28] and associated with cancer progression.[29] Since chemokines are often significantly upregulated during tumorigenesis and melanoma tumor cells secrete KC/CXCL-1,[30] which exerts signaling effects on endothelial cells, the significant reduction of KC/CXCL-1 suggests inhibition of tumor progression.

We then sectioned and stained tumor specimens with hematoxylin and eosin for pathology analysis of the tissues. Intriguingly, the percent of necrotic tissue within the tumor of the animals treated at the highest concentration of CVS-16 (**10b**) (40-50 mg/kg) had significantly more necrosis than control ($^{**}p<0.01$) and 20 mg/kg treated animals ($^{*}p<0.05$) (Fig. 6D). In addition, the endothelial cells and state of the tumor specimens was examined. One hundred percent of the control specimens contained viable endothelial cells. This was in contrast to 20 mg/kg treated animals, of which 50% contained only viable endothelial cells present and the other 50% of specimens displayed mixed areas with viable endothelial cells and also necrotic endothelial cells (Fig. 6E). Most interesting was that 100% of specimens from animals treated with 40–50 mg/kg of CVS-16 (**10b**) contained necrotic endothelial cells in close proximity to necrotic malignant cells. Taken together, the data suggests an anti-angiogenesis

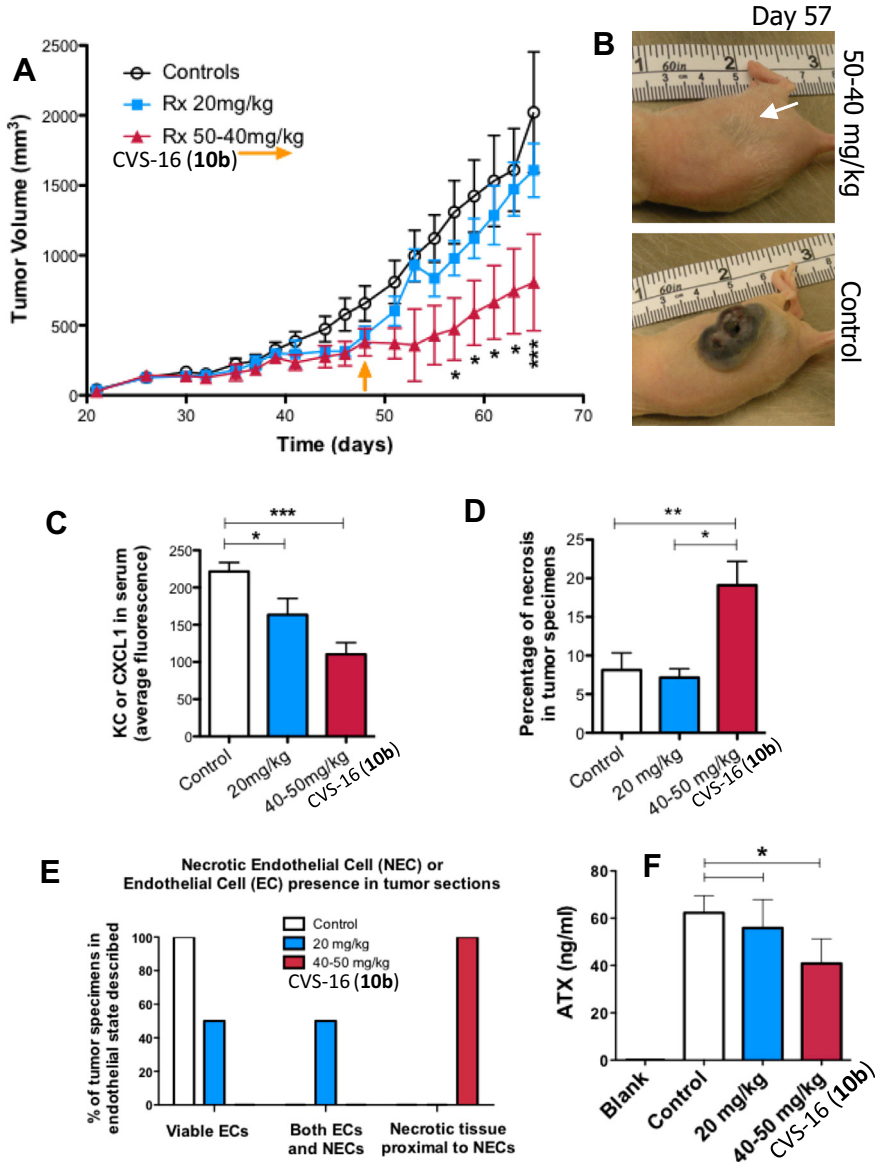

Figure 6. CVS-16 (**10b**) blunts tumor progression by inhibiting angiogenesis in a melanoma xenograft model. (A) Animals with melanoma tumors were treated with the indicated concentrations of CVS-16 (**10b**) and established tumors were measured with calipers every other day. The arrow indicates the reduction of dosage from 50 mg/kg to 40 mg/kg on day 47 (see text for details). $^{*}p<0.05$ and $^{***}p<0.001$, control ($n = 10$) versus 50–40 mg/kg ($n = 5$). There was no significant difference among the control group ($n = 10$) versus 20 mg/kg ($n = 5$). (B) Images of tumors on day 57 from control and treated animals. (C) Serum was collected and analyzed for KC/CXCL1. $^{*}p<0.05$, control versus 20 mg/kg and $^{***}p<0.001$, control versus 50–40 mg/kg. (D) Quantification of specimens in the pathology report indicates the increase in tumor necrosis among animals treated with 50–40 mg/kg of CVS-16 (**10b**). $^{**}p<0.01$, control versus 40–50 mg/kg and $^{*}p<0.05$, 20 mg/kg versus 40–50 mg/kg. (E) Analysis of tumor specimens for regions with endothelial cells present indicates differences among the groups. (F) ATX was measured from the serum of treated and control animals. $^{*}p<0.05$, comparing drug treated animals to controls using ANOVA followed by the Bonferroni multiple comparison test.

mechanism of action for CVS-16 (**10b**). In support of this idea, we stained tumor sections with Ki-67 and detected no significant differences between specimens (data not shown).

In order to understand whether CVS-16 (**10b**) had biological activity in vivo, we isolated the mouse serum at necropsy for analysis of circulating ATX. We detected a significant reduction in the ATX of treated animals, compared to control (Fig. 6F, $^{*}p<0.05$ vs control). This suggests that CVS-16 (**10b**)-treated tumors manifested significant reduction in the expression and production of ATX. Taken together with the previous data, this indicates that the vinyl sulfone inhibits ATX which affects angiogenesis and melanoma progression in vivo.

Using the same in vivo model of melanoma progression, we also tested the efficacy of HA-130 and PF-8380. Surprisingly, neither of these ATX inhibitors reached statistical significance against the continuous growth of tumors from MeWo cell inoculation in mice (Fig. 7A and B). Upon necropsy, we collected the serum to analyze circulating ATX levels and observed no significant difference between the treated animals and the control group (Fig. 7C). This corroborated the results we observed with solid tumor growth, suggesting the compounds did not have a significant impact on ATX. Taken together, this further suggests that the vinyl sulfone CVS-16 (**10b**) has superior functional activity in comparison to these other ATX inhibitors.

4. Discussion

Herein we report the synthesis and biological activity of a vinyl sulfone analog of LPC, which acts as an active-site targeted irreversible inhibitor of ATX in vitro, and also shows activity against

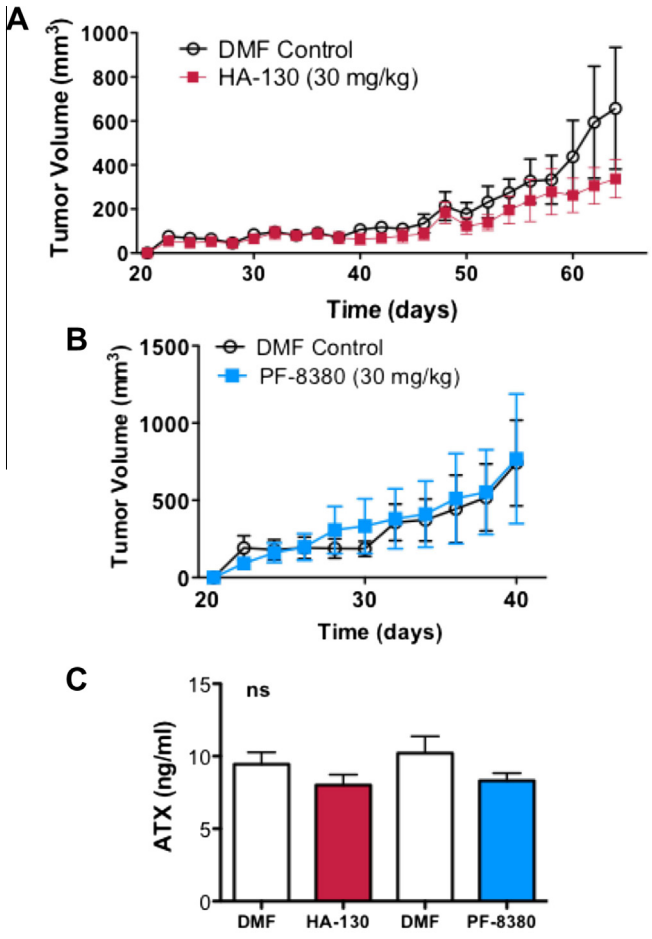

Figure 7. The autotaxin inhibitors HA-130 and PF-8380 did not impact tumor progression in a xenograft model of melanoma. Animals with melanoma tumors were treated with the indicated concentrations of either: HA-130 (A), PF-8380 (B) or dimethylformamide (DMF) solvent control. The established pigmented tumors were measured with calipers every other day. (C) ATX was measured from the serum of treated and control animals.

melanoma in vitro and in vivo. In addition to enzymatic inhibition of ATX by the vinyl sulfone analogs in vitro, we observed the reduction of cell viability and migration among multiple cancer cell types in vitro. Most importantly, we observed the inhibition of tumor progression using an in vivo model of melanoma and measured a reduction of ATX in the serum of treated animals. Taken together, our data suggests that the vinyl sulfone CVS-16 (**10b**) is a potent small molecule inhibitor of ATX with biological activity against its target, which reduces viability of cancer cells and inhibits angiogenesis necessary for tumor progression.

Our data also suggests that the vinyl sulfone CVS-16 (**10b**) compares very favorably against other compounds synthesized to inhibit ATX, like HA-130 and PF-8380. The first known inhibitor of ATX was L-histidine and it was limited in application due to the millimolar concentrations of L-histidine required to inhibit the lysophospholipase D activity of ATX.[15g] Later work identified alpha-halophosphonate analogs of LPA as potent ATX inhibitors,[31] as well as aromatic phosphonates.[15i,32] This report was the first to provide a proof-of-concept study that led to further innovation, as reviewed by Parrill, Baker and coworkers.[33] For example, using a chemical library screening approach and ~40,000 drug-like small molecules, thiazolidinediones were identified as ATX inhibitors that could be enhanced by the addition of a boronic acid moiety to achieve lower IC_{50} levels.[15a] Another screen of a small-molecule library yielded several ATX inhibitors, which lead to the synthesis of analogs based on their structural motifs and further validated ATX as a target for melanoma.[34]

We, and other groups, have also taken advantage of cyclic phosphatidic acid, a naturally occurring molecule that inhibits ATX and is an analog of ATX. Manipulating the compound structure to yield 3-carba analogs of cyclic phosphatidic acid produced potent inhibitors of ATX that were effective in vivo.[8a] Similarly, a phosphonothionate analog of carba cyclic phosphatidic acid also yielded a compound that inhibited the lysophospholipase D activity of ATX, the viability of melanoma cells and reduced melanoma metastasis in vivo.[8b] A recent study reported the evaluation of the stereoisomers of 3-carba cyclic phosphatidic acid, which are agonists of the LPA5 receptor, yet inhibit melanoma metastasis in vivo.[35]

There are several differences between these reports and the current inhibitor. First and foremost among these differences is the use of a vinyl sulfone moiety as a mild electrophile that is targeted to the active site by an alkyl chain and a quaternary ammonium derivative that recapitulate key recognition elements of the LPC substrate structure. As a result, CVS-16 (**10b**) is an irreversible, 'suicide' inhibitor of ATX. There is only one other reported irreversible inhibitor of ATX, a series of monofluoro- and difluoromethyl phenyl alkyl phosphodiesters that liberate a reactive quinone methide upon hydrolysis by ATX.[36] This irreversible inhibitor lacks the quaternary ammonium derivative for targeting, which we show is crucial for activity of the LPC-mimicking vinyl sulfones; lacking the quaternary ammonium derivative, analog PVS-16 (**21**) is essentially inactive. In addition, the reactive quinone methide is released as a diffusible highly reactive electrophile, rather that the more selective Thr-targeted vinyl sulfone.

Secondly, in previous studies we focused exclusively on advanced, metastatic models of melanoma using an allograft system.[8a,b] Herein, we established a solid xenograft melanoma tumor at one primary site, which is ideal for assessing the effects of angiogenesis. In this melanoma model, the tumors are highly pigmented, allowing for ease of visualization and measurements on nude mice. Our shift away from the highly metastatic allograft model is due to its poor reflection of human disease along with dubious conclusions that might be drawn from biological data derived by using it.[37]

Through the solid xenograft melanoma model, we discovered that the mechanism of action of CVS-16 (**10b**) in vivo is the reduction of angiogenesis, which is not what we had predicted based on the data gleaned from our in vitro studies. Since we detected reduced viability in the presence of CVS-16 (**10b**), we hypothesized that CVS-16 (**10b**) had a direct effect against tumor cells, possibly an inhibition of mitogenesis. However, mitogenesis inhibition is not what we observed in animals, rather it was angiogenesis inhibition. Interestingly, the angiogenic response of ATX was previously described as 'comparable to that elicited by VEGF'.[13a] Thus, our data is consistent with the known properties of ATX. Although we cannot completely rule out all other molecular mechanisms that may also contribute to this phenomenon, we can state that angiogenesis does not proceed in vivo, in the presence of 40–50 mg/kg CVS-16 (**10b**).

It is highly likely that 50 mg/kg (or very close to) is the MTD for CVS-16 (**10b**), certainly without pre-emptive supportive therapy for the animals. One treated mouse (50 mg/kg) died, presumably to the unspecified side effects of CVS-16 (**10b**) since it had only a miniscule-sized tumor and no obvious signs of metastases, even at necropsy. However, it is not uncommon to have 1 or 2 otherwise healthy, untreated mice in our animal colony die from dehydration for no obvious reason deduced by our veterinary staff. Nevertheless, the fact that a mouse possibly succumbed to side effects is consistent with the harsh adverse drug events manifested by angiogenesis inhibitors. For example, bevacizumab contains

several black-box warnings, which includes: fatal hemorrhage, increased arterial thromboembolic events (myocardial infarction and stroke), gastrointestinal perforation and complications to wound healing which requires discontinuation of the drug at least 28 days before surgery.[38] These black-box warnings are in addition to the other known drug toxicities of bevacizumab including hypertension, proteinuria and central nervous system events (e.g., dizziness, depression, headaches, seizure, lethargy, visual disturbances, etc.).[39]

Although adverse events are a concern for further pre-clinical development of ATX inhibitors, most anticancer therapeutics, in particular traditional, cytotoxic chemotherapy, produce harsh side effects for patients. However, this regrettable actuality is tolerated because of favorable therapeutic indexes and the potential for ameliorating a life-threatening illness. Even the newer classes of targeted biologics possess severe unwanted side effects, some even serving as a measure of therapeutic activity (e.g., an acne-like rash). Thus, there is extreme variability among patient compliance and tolerability of anticancer therapeutics, along with patients' willingness to continue therapy.

Although CVS-16 (**10b**) (40–50 mg/kg) was capable of sustaining an inhibition on tumor volume for approximately 53 days after the injection of tumor cells, the sizes of tumors in the highest treated group of animals started to increase on day 54. This was 6 days after we had reduced the dosage in this group from 50 mg/kg to 40 mg/kg. We cannot be certain whether this shift from static to growing tumors was due to the dosage reduction, chemoresistance or another factor. We did not observe any change in the amount of circulating VEGF among the treated mice in comparison to the controls (data not shown). This argues against a shift to VEGF or chemoresistance using this mechanism, which is what we had predicted since ATX works similarly to VEGF, and inhibiting both might be logically necessary to sustain a long-term response against tumor angiogenesis. Therefore, our supposition is that 50 mg/kg of CVS-16 (**10b**) is required for a sustained inhibition of ATX-dependent angiogenesis and tumor progression and that supportive care is required at this dosage.

Nevertheless, it was very exciting to observe the ability of CVS-16 (**10b**) to prevent melanoma tumor progression in animals. Advanced melanoma is a particularly difficult type of cancer to treat because it is unresponsive to traditional chemotherapy; therefore, immunotherapy is typically administered even though responses are achieved in less than 20% of patients. In the past few years, several new therapeutics for melanoma were approved for the first time in over a decade and these included trametinib, dabrafenib and vemurafenib. The drugs are intended for patients with activating BRAF mutations, which occurs in a majority of melanomas, but not all cases. Thus, more research is desperately needed to uncover drugs that can treat melanoma, especially since the incidence of this disease is rising. Besides melanoma, the compound was also effective against the viability and migration of MDA-MB-231 breast cells in vitro. This is very intriguing considering this cell line was isolated from the pleural effusion of a patient and represents a highly invasive triple-negative breast cancer, which is a clinically challenging subtype to treat. Taken together, our data supports further pre-clinical testing of the vinyl sulfone CVS-16 (**10b**) as an ATX inhibitor in a combination approach with other anticancer therapeutics against the progression of melanoma.

Acknowledgements

This work was supported in part by a Research Scholar Grant 120634 from the American Cancer Society (to M.M.M.), NS 29632 (to G.D.P.), HL 070231 (to G.D.P.) and the Georgia Research Alliance (to M.M.M.). G.W.J. would like to thank Schering-Plough/Merck for financial support during conduct of this project. M.M.M. would like to thank Caitlin Ruddick and Santosh Patel for their work in the laboratory. The following authors contributed to the design of the research study (M.M.M., G.W.J., D.M., G.D.P.), performed the research and collected data (M.M.M., G.W.J., M.K.A., W.J., D.T.N., J.M.F., H.T.N., S.K.T., A.A.A., D.M.), analyzed the data (M.M.M., G.W.J., M.A., W.J., D.T.N., W.J.H., D.M., G.D.P.) and wrote the paper (M.M.M., G.W.J., G.D.P.).

Supplementary data

Supplementary data associated with this article can be found, in the online version, at http://dx.doi.org/10.1016/j.bmc.2015.06.054.

References and notes

1. Umezu-Goto, M.; Kishi, Y.; Taira, A.; Hama, K.; Dohmae, N.; Takio, K.; Yamori, T.; Mills, G. B.; Inoue, K.; Aoki, J.; Arai, H. *J. Cell Biol.* **2002**, *158*, 227.
2. Murata, J.; Lee, H. Y.; Clair, T.; Krutzsch, H. C.; Arestad, A. A.; Sobel, M. E.; Liotta, L. A.; Stracke, M. L. *J. Biol. Chem.* **1994**, *269*, 30479.
3. Stracke, M. L.; Krutzsch, H. C.; Unsworth, E. J.; Arestad, A.; Cioce, V.; Schiffmann, E.; Liotta, L. A. *J. Biol. Chem.* **1992**, *267*, 2524.
4. (a) van Meeteren, L. A.; Ruurs, P.; Stortelers, C.; Bouwman, P.; van Rooijen, M. A.; Pradere, J. P.; Pettit, T. R.; Wakelam, M. J.; Saulnier-Blache, J. S.; Mummery, C. L.; Moolenaar, W. H.; Jonkers, J. *Mol. Cell. Biol.* **2006**, *26*, 5015; (b) Tanaka, M.; Okudaira, S.; Kishi, Y.; Ohkawa, R.; Iseki, S.; Ota, M.; Noji, S.; Yatomi, Y.; Aoki, J.; Arai, H. *J. Biol. Chem.* **2006**, *281*, 25822.
5. Fotopoulou, S.; Oikonomou, N.; Grigorieva, E.; Nikitopoulou, I.; Paparountas, T.; Thanassopoulou, A.; Zhao, Z.; Xu, Y.; Kontoyiannis, D. L.; Remboutsika, E.; Aidinis, V. *Dev. Biol.* **2010**, *339*, 451.
6. (a) Liu, S.; Murph, M.; Panupinthu, N.; Mills, G. B. *Cell Cycle* **2009**, *8*, 3695; (b) Liu, S.; Umezu-Goto, M.; Murph, M.; Lu, Y.; Liu, W.; Zhang, F.; Yu, S.; Stephens, L. C.; Cui, X.; Murrow, G.; Coombes, K.; Muller, W.; Hung, M. C.; Perou, C. M.; Lee, A. V.; Fang, X.; Mills, G. B. *Cancer Cell* **2009**, *15*, 539.
7. Nakai, Y.; Ikeda, H.; Nakamura, K.; Kume, Y.; Fujishiro, M.; Sasahira, N.; Hirano, K.; Isayama, H.; Tada, M.; Kawabe, T.; Komatsu, Y.; Omata, M.; Aoki, J.; Koike, K.; Yatomi, Y. *Clin. Biochem.* **2011**.
8. (a) Baker, D. L.; Fujiwara, Y.; Pigg, K. R.; Tsukahara, R.; Kobayashi, S.; Murofushi, H.; Uchiyama, A.; Murakami-Murofushi, K.; Koh, E.; Bandle, R. W.; Byun, H. S.; Bittman, R.; Fan, D.; Murph, M.; Mills, G. B.; Tigyi, G. *J. Biol. Chem.* **2006**, *281*, 22786; (b) Altman, M. K.; Gopal, V.; Jia, W.; Yu, S.; Hall, H.; Mills, G. B.; McGinnis, A. C.; Bartlett, M. G.; Jiang, G.; Madan, D.; Prestwich, G. D.; Xu, Y.; Davies, M. A.; Murph, M. M. *Mol. Cancer* **2010**, *9*, 140; (c) Singh, A. D.; Sisley, K.; Xu, Y.; Li, J.; Faber, P.; Plummer, S. J.; Mudhar, H. S.; Rennie, I. G.; Kessler, P. M.; Casey, G.; Williams, B. G. *Br. J. Ophthalmol.* **2007**, *91*, 1385.
9. Masuda, A.; Nakamura, K.; Izutsu, K.; Igarashi, K.; Ohkawa, R.; Jona, M.; Higashi, K.; Yokota, H.; Okudaira, S.; Kishimoto, T.; Watanabe, T.; Koike, Y.; Ikeda, H.; Kozai, Y.; Kurokawa, M.; Aoki, J.; Yatomi, Y. *Br. J. Haematol.* **2008**, *143*, 60.
10. Kishi, Y.; Okudaira, S.; Tanaka, M.; Hama, K.; Shida, D.; Kitayama, J.; Yamori, T.; Aoki, J.; Fujimaki, T.; Arai, H. *J. Biol. Chem.* **2006**, *281*, 17492.
11. Tokumura, A.; Kume, T.; Fukuzawa, K.; Tahara, M.; Tasaka, K.; Aoki, J.; Arai, H.; Yasuda, K.; Kanzaki, H. *Life Sci.* **2007**, *80*, 1641.
12. Samadi, N.; Gaetano, C.; Goping, I. S.; Brindley, D. N. *Oncogene* **2009**, *28*, 1028.
13. (a) Nam, S. W.; Clair, T.; Kim, Y. S.; McMarlin, A.; Schiffmann, E.; Liotta, L. A.; Stracke, M. L. *Cancer Res.* **2001**, *61*, 6938; (b) Ptaszynska, M. M.; Pendrak, M. L.; Stracke, M. L.; Roberts, D. D. *Mol. Cancer Res.* **2010**, *8*, 309.
14. Ptaszynska, M. M.; Pendrak, M. L.; Bandle, R. W.; Stracke, M. L.; Roberts, D. D. *Mol. Cancer Res.* **2008**, *6*, 352.
15. (a) Albers, H. M.; Dong, A.; van Meeteren, L. A.; Egan, D. A.; Sunkara, M.; van Tilburg, E. W.; Schuurman, K.; van Tellingen, O.; Morris, A. J.; Smyth, S. S.; Moolenaar, W. H.; Ovaa, H. *Proc. Natl. Acad. Sci. U.S.A.* **2010**, *107*, 7257; (b) Gierse, J.; Thorarensen, A.; Beltey, K.; Bradshaw-Pierce, E.; Cortes-Burgos, L.; Hall, T.; Johnston, A.; Murphy, M.; Nemirovskiy, O.; Ogawa, S.; Pegg, L.; Pelc, M.; Prinsen, M.; Schnute, M.; Wendling, J.; Wene, S.; Weinberg, R.; Wittwer, A.; Zweifel, B.; Masferrer, J. *J. Pharmacol. Exp. Ther.* **2010**, *334*, 310; (c) Hoeglund, A. B.; Bostic, H. E.; Howard, A. L.; Wanjala, I. W.; Best, M. D.; Baker, D. L.; Parrill, A. L. *J. Med. Chem.* **2010**, *53*, 1056; (d) Xu, X.; Yang, G.; Zhang, H.; Prestwich, G. D. *Prostaglandins Other Lipid Mediat.* **2009**, *89*, 140; (e) Zhang, H.; Xu, X.; Gajewiak, J.; Tsukahara, R.; Fujiwara, Y.; Liu, J.; Fells, J. I.; Perygin, D.; Parrill, A. L.; Tigyi, G.; Prestwich, G. D. *Cancer Res.* **2009**, *69*, 5441; (f) Ferry, G.; Moulharat, N.; Pradere, J. P.; Desos, P.; Try, A.; Genton, A.; Giganti, A.; Beucher-Gaudin, M.; Lonchampt, M.; Bertrand, M.; Saulnier-Blache, J. S.; Tucker, G. C.; Cordi, A.; Boutin, J. A. *J. Pharmacol. Exp. Ther.* **2008**, *327*, 809; (g) Clair, T.; Koh, E.; Ptaszynska, M.; Bandle, R. W.; Liotta, L. A.; Schiffmann, E.; Stracke, M. L. *Lipids Health Dis.* **2005**, *4*, 5; (h) East, J. E.; Kennedy, A. J.; Tomsig, J. L.; De Leon, A. R.; Lynch, K. R.; Macdonald, T. L. *Bioorg. Med. Chem. Lett.* **2010**, *20*, 7132; (i) Gupte, R.; Patil, R.; Liu, J.; Wang, Y.; Lee, S. C.; Fujiwara, Y.; Fells, J.; Bolen, A. L.; Emmons-Thompson, K.; Yates, C. R.; Siddam, A.; Panupinthu, N.; Pham, T. C.; Baker, D. L.; Parrill, A. L.; Mills, G. B.; Tigyi, G.; Miller, D. D. *ChemMedChem* **2011**; (j) Prestwich, G. D.; Gajewiak, J.; Zhang, H.; Xu, X.; Yang, G.; Serban, M. *Biochim. Biophys. Acta* **2008**, *1781*, 588; (k) Durgam, G. G.; Virag, T.; Walker, M.

D.; Tsukahara, R.; Yasuda, S.; Liliom, K.; van Meeteren, L. A.; Moolenaar, W. H.; Wilke, N.; Siess, W.; Tigyi, G.; Miller, D. D. *J. Med. Chem.* **2005**, *48*, 4919; (l) Albers, H. M.; Ovaa, H. *Chem. Rev.* **2012**, *112*, 2593; (m) St-Coeur, P. D.; Ferguson, D.; Morin, P., Jr.; Touaibia, M. *Arch. Pharm. (Weinheim)* **2013**, *346*, 91.
16. Ueda, K.; Yoshihara, M.; Nakao, M.; Tanaka, T.; Sano, S.; Fukuzawa, K.; Tokumura, A. *J. Agric. Food Chem.* **2010**, *58*, 6053.
17. van Meeteren, L. A.; Ruurs, P.; Christodoulou, E.; Goding, J. W.; Takakusa, H.; Kikuchi, K.; Perrakis, A.; Nagano, T.; Moolenaar, W. H. *J. Biol. Chem.* **2005**, *280*, 21155.
18. Nishimasu, H.; Okudaira, S.; Hama, K.; Mihara, E.; Dohmae, N.; Inoue, A.; Ishitani, R.; Takagi, J.; Aoki, J.; Nureki, O. *Nat. Struct. Mol. Biol.* **2011**, *18*, 205.
19. Hausmann, J.; Kamtekar, S.; Christodoulou, E.; Day, J. E.; Wu, T.; Fulkerson, Z.; Albers, H. M.; van Meeteren, L. A.; Houben, A. J.; van Zeijl, L.; Jansen, S.; Andries, M.; Hall, T.; Pegg, L. E.; Benson, T. E.; Kasiem, M.; Harlos, K.; Kooi, C. W.; Smyth, S. S.; Ovaa, H.; Bollen, M.; Morris, A. J.; Moolenaar, W. H.; Perrakis, A. *Nat. Struct. Mol. Biol.* **2011**, *18*, 198.
20. Powers, J. C.; Asgian, J. L.; Ekici, O. D.; James, K. E. *Chem. Rev.* **2002**, *102*, 4639.
21. (a) Hanzlik, R. P.; Thompson, S. A. *J. Med. Chem.* **1984**, *27*, 711; (b) Cormack, Mc. *J. Biol. Chem.* **1997**, *272*, 26103.
22. Bogyo, M.; McMaster, J. S.; Gaczynska, M.; Tortorella, D.; Goldberg, A. L.; Ploegh, H. *Proc. Natl. Acad. Sci. U.S.A.* **1997**, *94*, 6629.
23. Nguyen, D.; Nguyen, O.; Zhang, H.; Prestwich, G. D.; Murph, M. M. A Bromophosphonate Analogue of Lysophosphatidic Acid Surpasses Dacarbazine in Reducing Cell Proliferation and Viability of MeWo Melanoma Cells. In *Research on Melanoma—A Glimpse into Current Directions and Future Trends*; Murph, M. M., Ed.; InTech, 2011.
24. Xu, X.; Prestwich, G. D. *Cancer* **2010**, *116*, 1739.
25. Ferguson, C. G.; Bigman, C. S.; Richardson, R. D.; van Meeteren, L. A.; Moolenaar, W. H.; Prestwich, G. D. *Org. Lett.* **2006**, *8*, 2023.
26. (a) Luquain, C.; Sciorra, V. A.; Morris, A. J. *Trends Biochem. Sci.* **2003**, *28*, 377; (b) Moolenaar, W. H. *J. Biol. Chem.* **1995**, *270*, 12949.
27. North, E. J.; Osborne, D. A.; Bridson, P. K.; Baker, D. L.; Parrill, A. L. *Bioorg. Med. Chem.* **2009**, *17*, 3433.
28. Lee, Z.; Swaby, R. F.; Liang, Y.; Yu, S.; Liu, S.; Lu, K. H.; Bast, R. C., Jr.; Mills, G. B.; Fang, X. *Cancer Res.* **2006**, *66*, 2740.
29. Loukinova, E.; Dong, G.; Enamorado-Ayalya, I.; Thomas, G. R.; Chen, Z.; Schreiber, H.; Van Waes, C. *Oncogene* **2000**, *19*, 3477.
30. Richmond, A.; Yang, J.; Su, Y. *Pigment Cell Melanoma Res.* **2009**, *22*, 175.
31. Jiang, G.; Xu, Y.; Fujiwara, Y.; Tsukahara, T.; Tsukahara, R.; Gajewiak, J.; Tigyi, G.; Prestwich, G. D. *ChemMedChem* **2007**, *2*, 679.
32. Jiang, G.; Madan, D.; Prestwich, G. D. *Bioorg. Med. Chem. Lett.* **2011**, *21*, 5098.
33. (a) Parrill, A. L.; Baker, D. L. *Expert Opin. Ther. Pat.* **2010**, *20*, 1619; (b) Norman, D. D.; Ibezim, A.; Scott, W. E.; White, S.; Parrill, A. L.; Baker, D. L. *Bioorg. Med. Chem.* **2013**, *21*, 5548.
34. Saunders, L. P.; Ouellette, A.; Bandle, R.; Chang, W. C.; Zhou, H.; Misra, R. N.; De La Cruz, E. M.; Braddock, D. T. *Mol. Cancer Ther.* **2008**, *7*, 3352.
35. Gupte, R.; Siddam, A.; Lu, Y.; Li, W.; Fujiwara, Y.; Panupinthu, N.; Pham, T. C.; Baker, D. L.; Parrill, A. L.; Gotoh, M.; Murakami-Murofushi, K.; Kobayashi, S.; Mills, G. B.; Tigyi, G.; Miller, D. D. *Bioorg. Med. Chem. Lett.* **2010**, *20*, 7525.
36. Parrill, A. L.; Baker, D. L.; Montedonico, L. E. Mechanism-Based Inactivators of Autotaxin 2011.
37. Herlyn, M.; Fukunaga-Kalabis, M. *J. Invest. Dermatol.* **2010**, *130*, 911.
38. *Avastin (bevacizumab)* [package insert]; Genentech, Inc. A Member of the Roche Group: South San Francisco, CA; 2015.
39. Chu, E.; DeVita, V. T. *Physicians' Cancer Chemotherapy Drug Manual*; Jones and Bartlett Publishers: Sudbury, MA, 2011. p 591.